

Domain Adaptation with Conditional Distribution Matching and Generalized Label Shift

Remi Tachet des Combes^{†*}, Han Zhao^{‡*}, Yu-Xiang Wang[◇], Geoffrey J. Gordon^{†,‡}

[†]Microsoft Research Montreal, [‡]Carnegie Mellon University, [◇]UC Santa Barbara
{retachet, ggordon}@microsoft.com, han.zhao@cs.cmu.edu, yuxiangw@cs.ucsb.edu

Abstract

Adversarial learning has demonstrated good performance in the unsupervised domain adaptation setting, by learning domain-invariant representations that perform well on the source domain. However, recent work has underlined limitations of existing methods in the presence of mismatched label distributions between the source and target domains. In this paper, we extend a recent upper-bound on the performance of adversarial domain adaptation to multi-class classification and more general discriminators. We then propose *generalized label shift (GLS)* as a way to improve robustness against mismatched label distributions. *GLS* states that, conditioned on the label, there exists a representation of the input that is invariant between the source and target domains. Under *GLS*, we provide theoretical guarantees on the transfer performance of any classifier. We also devise necessary and sufficient conditions for *GLS* to hold. The conditions are based on the estimation of the relative class weights between domains and on an appropriate reweighting of samples. Guided by our theoretical insights, we modify three widely used algorithms, JAN, DANN and CDAN and evaluate their performance on standard domain adaptation tasks where our method outperforms the base versions. We also demonstrate significant gains on artificially created tasks with large divergences between their source and target label distributions.

1 Introduction

In spite of impressive successes, most deep learning models (Goodfellow et al., 2017) rely on huge amounts of labelled data and their features have proven brittle to distribution shifts (Yosinski et al., 2014; McCoy et al., 2019). Building more robust models, that learn from fewer samples and/or generalize better out-of-distribution is the focus of many recent works (Bachman et al., 2019; Arjovsky et al., 2019; Yaghoobzadeh et al., 2019). The research direction of interest to this paper is that of domain adaptation, which aims at learning features that transfer well between domains.

We focus in particular on the unsupervised domain adaptation setting (UDA), where the algorithm has access to labelled samples from a source domain and unlabelled data from a target domain. Its objective is to train a model that generalizes well to the target domain. Building on advances in adversarial learning (Goodfellow et al., 2014), adversarial domain adaptation (ADA) leverages the use of a discriminator to learn an intermediate representation that is invariant between the source and target domains. Simultaneously, the representation is paired with a classifier, trained to perform well on the source domain (Ganin et al., 2016; Tzeng et al., 2017; Zhao et al., 2018b; Liu et al., 2019). ADA is rather successful on a variety of tasks, however, recent work

*Equal Contribution

has proven an upper bound on the performance of existing algorithms when source and target domains have mismatched label distributions (Zhao et al., 2019b). Label, or prior probability, shift is a property of two domains for which the marginal label distributions differ, but the conditional distributions of input given label stay the same across domains (Storkey, 2009; Zhang et al., 2015).

In this paper, we study domain adaptation under mismatched label distributions and design methods that are robust in that setting. Our contributions are the following. First, we extend the upper bound by Zhao et al. (2019b) to k -class classification and to conditional domain adversarial networks, a recently introduced domain adaptation algorithm (Long et al., 2018). Second, we introduce *generalized label shift (GLS)*, a broader version of the standard label shift where conditional invariance between source and target domains is placed in representation rather than input space. Third, we derive performance guarantees for algorithms that seek to enforce *GLS* via learnt feature transformations, in the form of upper bounds on the error gap and the joint error of the classifier on the source and target domains. Those performance guarantees suggest principled modifications to ADA to improve its robustness to mismatched label distributions. The modifications rely on estimating the class ratios between source and target domains and use those as importance weights in the adversarial and classification objectives. The importance weights estimation is performed using a method from Lipton et al. (2018). Following the theoretical insights, we devise three new algorithms, based on DANNs (Ganin et al., 2016), JANs (Long et al., 2017) and CDANs (Long et al., 2018). We apply our variants to artificial UDA tasks with large divergences between label distributions, and demonstrate significant performance gains compared to the algorithms’ base versions. Finally, we evaluate them on standard domain adaptation tasks (for which the divergence between label distribution is rather limited) and show improved performance as well.

2 Preliminary

Notations In this paper we focus on the general k -class classification problem. We use \mathcal{X} and \mathcal{Y} to denote the input and output space, respectively. Similarly, \mathcal{Z} stands for the representation space induced from \mathcal{X} by a feature transformation $g : \mathcal{X} \mapsto \mathcal{Z}$. Accordingly, we use X, Y, Z to denote random variables which take values in $\mathcal{X}, \mathcal{Y}, \mathcal{Z}$. In this work, *domain* corresponds to a distribution on the input space \mathcal{X} and output space \mathcal{Y} , and we use \mathcal{D}_S (resp. \mathcal{D}_T) to denote the source (resp. target) domain. Noticeably, this corresponds to a stochastic setting, which is stronger than the deterministic one studied in Ben-David et al. (2007, 2010); Zhao et al. (2019b). A *hypothesis* is a function $h : \mathcal{X} \rightarrow [k]$. The *error* of a hypothesis h under distribution \mathcal{D}_S is defined as: $\varepsilon_S(h) := \Pr_{\mathcal{D}_S}(h(X) \neq Y)$, i.e., the probability that h disagrees with Y under \mathcal{D}_S .

Domain Adaptation via Invariant Representations For source (\mathcal{D}_S) and target (\mathcal{D}_T) domains, we use $\mathcal{D}_S^X, \mathcal{D}_T^X, \mathcal{D}_S^Y$ and \mathcal{D}_T^Y to denote the marginal data and label distributions. In UDA, the algorithm has access to n labeled points $\{(\mathbf{x}_i, y_i)\}_{i=1}^n \in (\mathcal{X} \times \mathcal{Y})^n$ and m unlabeled points $\{\mathbf{x}_j\}_{j=1}^m \in \mathcal{X}^m$ sampled i.i.d. from the source and target domains. Inspired by Ben-David et al. (2010), a common approach is to learn representations invariant to the domain shift. Letting $g : \mathcal{X} \mapsto \mathcal{Z}$ be a feature transformation and $h : \mathcal{Z} \mapsto \mathcal{Y}$ a hypothesis on the feature space, the goal of domain invariant representations (Ganin et al., 2016; Tzeng et al., 2017; Zhao et al., 2018a) is to find a function g that induces similar distributions on \mathcal{D}_S and \mathcal{D}_T . Simultaneously, g is required to preserve rich information about the target task so that $\varepsilon_S(h \circ g)$ is small. The above process results in the following Markov chain:

$$X \xrightarrow{g} Z \xrightarrow{h} \hat{Y}, \quad (1)$$

with $\hat{Y} = h(g(X))$. We let $\mathcal{D}_S^Z, \mathcal{D}_T^Z, \mathcal{D}_S^{\hat{Y}}$ and $\mathcal{D}_T^{\hat{Y}}$ denote the pushforwards of \mathcal{D}_S and \mathcal{D}_T by g and $h \circ g$. Invariance in feature space is defined as minimizing a distance or divergence between the source and target

feature distributions.

Table 1: Common assumptions in the domain adaptation literature.

Covariate Shift	Label Shift
$\mathcal{D}_S^X \neq \mathcal{D}_T^X$	$\mathcal{D}_S^Y \neq \mathcal{D}_T^Y$
$\forall \mathbf{x} \in \mathcal{X}, \mathcal{D}_S(Y X = \mathbf{x}) = \mathcal{D}_T(Y X = \mathbf{x})$	$\forall y \in \mathcal{Y}, \mathcal{D}_S(X Y = y) = \mathcal{D}_T(X Y = y)$

Adversarial Domain Adaptation Invariance is often attained by training a discriminator $d : \mathcal{Z} \mapsto [0, 1]$ to predict whether a representation z is from the source or target domain. g is then trained both to maximize the discriminator loss and to minimize the classification loss of $h \circ g$ on the source domain (h is also trained with the latter objective).

This leads in particular to domain-adversarial neural networks (Ganin et al., 2016, DANN), where g , h and d are parameterized with neural networks: g_θ , h_ϕ and d_ψ . d_ψ outputs the probability to be from the source domain, while h_ϕ outputs the probability to belong to each class. The discriminator loss \mathcal{L}_{DA} and classification loss \mathcal{L}_C are simply cross-entropies. d_ψ , resp. g_θ , are then trained to minimize, resp. maximize \mathcal{L}_{DA} , while h_ϕ and g_θ minimize \mathcal{L}_C (see Algo. 1 and App. B.4 for details).

Building on DANN, conditional domain adversarial networks (Long et al., 2018, CDAN) use the same adversarial paradigm. However, the discriminator now takes as input the outer product, for a given x , between the predictions of the network $h(g(x))$ and its representation $g(x)$. In other words, d acts on the outer product:

$$h \otimes g(x) := (h_1(g(x)) \cdot g(x), \dots, h_k(g(x)) \cdot g(x))$$

rather than on $g(x)$ (where h_i denotes the i -th element of vector h). We now highlight a limitation of DANNs and CDANs.

An Information-Theoretic Lower Bound Let D_{JS} denote the Jensen-Shanon divergence between two distributions (see App. A.1 for details), and let \tilde{Z} correspond to Z (for DANN) or to $\hat{Y} \otimes Z$ (for CDAN). The following theorem gives a lower bound on the joint error of the classifier on the source and target domains:

Theorem 2.1. Suppose that the Markov chain in (1) holds, and that $D_{JS}(\mathcal{D}_S^Y \parallel \mathcal{D}_T^Y) \geq D_{JS}(\mathcal{D}_S^{\tilde{Z}} \parallel \mathcal{D}_T^{\tilde{Z}})$, then:

$$\varepsilon_S(h \circ g) + \varepsilon_T(h \circ g) \geq \frac{1}{2} \left(\sqrt{D_{JS}(\mathcal{D}_S^Y \parallel \mathcal{D}_T^Y)} - \sqrt{D_{JS}(\mathcal{D}_S^{\tilde{Z}} \parallel \mathcal{D}_T^{\tilde{Z}})} \right)^2.$$

Remark Remarkably, the above lower bound is algorithm-independent. It is also a population-level result and holds asymptotically with increasing data; large data does not help. Zhao et al. (2019b) prove the theorem for $k = 2$ and $\tilde{Z} = Z$, i.e., for DANN on binary classification. We extend it to CDAN and arbitrary k (see App. A.3 for the proof). Assuming that label distributions differ between source and target domains, the lower bound in Theorem 2.1 says that:

For both DANN and CDAN, the better the alignment of marginal feature distributions, the worse the sum of errors on source and target domains.

Notably, for an invariant representation ($D_{JS}(\mathcal{D}_S^{\bar{Z}}, \mathcal{D}_T^{\bar{Z}}) = 0$) with no source error, the target error will be larger than $D_{JS}(\mathcal{D}_S^Y, \mathcal{D}_T^Y)/2$. Put another way, algorithms learning invariant representations and minimizing the source empirical risk are fundamentally flawed when marginal label distributions differ between source and target domains.

Intuitively, CDAN also suffers from an intrinsic lower bound because while its discriminator d takes into account the predicted output distribution, \hat{Y} is still a function of X^1 . All the information available to the discriminator comes from X . From an information-theoretic perspective, to circumvent the above tradeoff between distribution alignment and target error minimization, it is necessary to incorporate the ground-truth label distributions (\mathcal{D}_S^Y and \mathcal{D}_T^Y) into the discriminator.

Common Assumptions to Tackle Domain Adaptation Domain adaptation requires assumptions about the data to be possible. Two common ones are *covariate shift* and *label shift*. They correspond to different ways of decomposing the joint distribution over $X \times Y$, as detailed in Table 1. From the perspective of representation learning, it has been demonstrated that covariate shift is not robust to feature transformation, and can lead to an effect called negative transfer (Zhao et al., 2019b). At the same time, label shift clearly fails in most practical applications. Consider, for instance, transferring knowledge from synthetic to real images (Visda, 2017): the supports of the input distributions are actually disjoint. In this paper, we focus on label shift and propose a solution to the above problem.

3 Main Results

In light of the limitations of existing assumptions, (e.g. covariate shift and label shift), we propose *generalized label shift* (GLS), a relaxation of label shift that substantially improves its applicability. We first discuss some of its properties and explain why the assumption is favorable in domain adaptation based on representation learning. Motivated by GLS, we then present a novel error decomposition theorem that directly suggests a bound minimization framework for domain adaptation. The framework is naturally compatible with \mathcal{F} -integral probability metrics (Müller, 1997, \mathcal{F} -IPM) and generates a family of domain adaptation algorithms by choosing various function classes \mathcal{F} . In a nutshell, the proposed framework applies Lipton et al. (2018)’s method-of-moments to estimate the importance weight \mathbf{w} of the *marginal label distributions* by solving a quadratic program (QP), and then uses \mathbf{w} to align the weighted source feature distribution with the target feature distribution.

3.1 Generalized Label Shift

Definition 3.1 (Generalized Label Shift, GLS). A representation $Z = g(X)$ satisfies GLS if

$$\mathcal{D}_S(Z \mid Y = y) = \mathcal{D}_T(Z \mid Y = y), \forall y \in \mathcal{Y}. \quad (2)$$

First, we note that when g is the identity map, i.e. $Z = X$, the above definition of GLS reduces to the original label shift assumption. Next, GLS is always achievable for any distribution pair $(\mathcal{D}_S, \mathcal{D}_T)$: any constant function $g \equiv c \in \mathbb{R}$ satisfies the above definition. The most important property of GLS is arguably that, unlike label shift, the above definition is compatible with a perfect classifier in the noiseless case. More specifically, suppose there exists a ground-truth labeling function h^* such that $Y = h^*(X)$; then h^* satisfies GLS. As a comparison, without conditioning on $Y = y$, the optimal labeling function does not satisfy

¹Th.2.1 actually holds for any \bar{Z} s.t. $\hat{Y} = \tilde{h}(\bar{Z})$, see App. A.3.

$\mathcal{D}_S(h^*(X)) = \mathcal{D}_T(h^*(X))$ if the marginal label distributions are different across domains. This observation is also consistent with the lower bound in Theorem 2.1, which holds for arbitrary marginal label distributions. *GLS* imposes label shift in the feature space \mathcal{Z} instead of the original input space \mathcal{X} . Conceptually, although samples from the same classes in the source and target domain can be dramatically different, the hope is to find an intermediate representation for both domains in which samples from a given class look similar to one another. Taking digit classification as an example and assuming the feature variable Z corresponds to the contour of a digit, it is possible that by using different contour extractors for e.g. MNIST and USPS, those contours look roughly the same in both domains. Technically, *GLS* can be facilitated by having separate representation extractors g_S and g_T for source and target² (Bousmalis et al., 2016; Tzeng et al., 2017).

3.2 An Error Decomposition Theorem based on *GLS*

Before delving into practical ways to enforce *GLS*, we provide performance guarantees for models that satisfy it, in the form of upper bounds on the error gap and on the joint error between source and target domains. The bound requires the following two concepts:

Definition 3.2 (Balanced Error Rate). The *balanced error rate* (BER) of predictor \hat{Y} on domain \mathcal{D}_S is:

$$\text{BER}_{\mathcal{D}_S}(\hat{Y} \parallel Y) := \max_{j \in [k]} \mathcal{D}_S(\hat{Y} \neq Y | Y = j). \quad (3)$$

Definition 3.3 (Conditional Error Gap). Given a joint distribution \mathcal{D} , the *conditional error gap* of a classifier \hat{Y} is $\Delta_{\text{CE}}(\hat{Y}) := \max_{y \neq y' \in \mathcal{Y}^2} |\mathcal{D}_S(\hat{Y} = y' | Y = y) - \mathcal{D}_T(\hat{Y} = y' | Y = y)|$.

When *GLS* and (1) hold, the conditional error gap is equal to 0. The next theorem gives an upper bound on the error gap between source and target; it can also be used to obtain a generalization upper bound on the target risk.

Theorem 3.1. (Error Decomposition Theorem) For any classifier $\hat{Y} = (h \circ g)(X)$,

$$|\varepsilon_S(h \circ g) - \varepsilon_T(h \circ g)| \leq \|\mathcal{D}_S^Y - \mathcal{D}_T^Y\|_1 \cdot \text{BER}_{\mathcal{D}_S}(\hat{Y} \parallel Y) + 2(k-1)\Delta_{\text{CE}}(\hat{Y}),$$

where $\|\mathcal{D}_S^Y - \mathcal{D}_T^Y\|_1 := \sum_{i=1}^k |\mathcal{D}_S(Y = i) - \mathcal{D}_T(Y = i)|$ is the L_1 distance between \mathcal{D}_S^Y and \mathcal{D}_T^Y .

Remark The upper bound in Theorem 3.1 provides a way to decompose the error gap between source and target domains. Additionally, with such a bound, we can immediately obtain a generalization bound of the target risk $\varepsilon_T(h)$. The upper bound contains two terms. The first one, $\|\mathcal{D}_S^Y - \mathcal{D}_T^Y\|_1$, measures the distance between the marginal label distributions across domains, and is a constant that only depends on the adaptation problem itself. It also contains BER, a reweighted classification performance on the source domain. The second term, $\Delta_{\text{CE}}(\hat{Y})$, by definition, measures the distance between the family of conditional distributions $\hat{Y} | Y$. In other words, the above upper bound is oblivious to the optimal labeling functions in feature space. This is in sharp contrast with upper bounds from previous work (Ben-David et al., 2010, Theorem 2), (Zhao et al., 2019b, Theorem 4.1), which essentially decompose the error gap in terms of the distance between the marginal feature distributions ($\mathcal{D}_S^Z, \mathcal{D}_T^Z$) and the optimal labeling functions (f_S^Z, f_T^Z). Because the optimal labeling function in feature space depends on Z and is unknown in practice, such decomposition is not very informative. As a comparison, Theorem 3.1 provides a decomposition orthogonal to previous results and does not require knowledge about unknown optimal labeling functions in feature space.

²For $\mathbf{x} \in \mathcal{D}_S$ (resp. $\mathbf{x} \in \mathcal{D}_T$), $z = g_S(\mathbf{x})$ (resp. $z = g_T(\mathbf{x})$).

Notably, the balanced error rate, $\text{BER}_{\mathcal{D}_S}(\hat{Y} \parallel Y)$, only depends on samples from the source domain, hence we can seek to minimize it in order to minimize the upper bound. Furthermore, using a data-processing argument, the conditional error gap $\Delta_{\text{CE}}(\hat{Y})$, can be minimized by aligning the conditional feature distributions across domains. Putting everything together, the upper bound on the error difference between source and target domains suggests that, in order to minimize the error gap, it suffices to align the conditional distributions $Z \mid Y = y$ while simultaneously minimizing the balanced error rate. In fact, under the assumption that the conditional distributions are perfectly aligned (i.e., under *GLS*), we can prove a stronger result, guaranteeing that the joint error is small:

Theorem 3.2. If $Z = g(X)$ satisfies *GLS*, then for any $h : \mathcal{Z} \rightarrow \mathcal{Y}$ and letting $\hat{Y} = h(Z)$ be the predictor, we have $\varepsilon_S(\hat{Y}) + \varepsilon_T(\hat{Y}) \leq 2\text{BER}_{\mathcal{D}_S}(\hat{Y} \parallel Y)$.

Remark Theorems 3.1 and 3.2 imply that if the conditional feature distributions are aligned, then both the source and target error will be bounded by $\text{BER}_{\mathcal{D}_S}(\hat{Y} \parallel Y)$. This suggests seeking models that simultaneously verify *GLS* and minimize $\text{BER}_{\mathcal{D}_S}(\hat{Y} \parallel Y)$. Since the balanced error rate only depends on the source domain, using labeled samples from the source domain is sufficient to minimize it.

3.3 Conditions for Generalized Label Shift

The main difficulty in applying a bound minimization algorithm inspired by Theorem 3.1 is that we do not have access to labels from the target domain in UDA³, so we cannot directly align the conditional label distributions. Below, we provide a necessary condition for *GLS* that avoids the need to explicitly align the conditional feature distributions.

Definition 3.4. Assuming $\mathcal{D}_S(Y = y) > 0, \forall y \in \mathcal{Y}$, we let $\mathbf{w} \in \mathbb{R}^k$ denote the importance weights of the target and source label distributions:

$$\mathbf{w}_y := \frac{\mathcal{D}_T(Y = y)}{\mathcal{D}_S(Y = y)}, \quad \forall y \in \mathcal{Y}. \quad (4)$$

Given the importance weights vector, a necessary condition implied by *GLS* is expressed in the following lemma.

Lemma 3.1. Assuming $Z = g(X)$ satisfies *GLS*, then $\mathcal{D}_T(Z) = \sum_{y \in \mathcal{Y}} \mathbf{w}_y \cdot \mathcal{D}_S(Z, Y = y) =: \mathcal{D}_S^{\mathbf{w}}(Z)$.

Compared to previous work that attempts to align $\mathcal{D}_T(Z)$ with $\mathcal{D}_S(Z)$ using adversarial discriminators (Ganin et al., 2016) or maximum mean discrepancy (MMD) (Long et al., 2015), Lemma 3.1 suggests that we should instead align $\mathcal{D}_T(Z)$ with the *reweighted* marginal distribution $\mathcal{D}_S^{\mathbf{w}}(Z)$.

Reciprocally, one may be interested to know when perfectly aligned target feature distribution and reweighted source feature distribution imply *GLS*. The following theorem gives a sufficient condition to answer this question:

Theorem 3.3. (Clustering structure implies sufficiency) Let $Z = g(X)$ such that $\mathcal{D}_T(Z) = \mathcal{D}_S^{\mathbf{w}}(Z)$. Assume $\mathcal{D}_T(Y = y) > 0, \forall y \in \mathcal{Y}$. If there exists a partition of $\mathcal{Z} = \cup_{y \in \mathcal{Y}} \mathcal{Z}_y$ such that $\forall y \in \mathcal{Y}$, $\mathcal{D}_S(Z \in \mathcal{Z}_y \mid Y = y) = \mathcal{D}_T(Z \in \mathcal{Z}_y \mid Y = y) = 1$, then $Z = g(X)$ satisfies *GLS*.

³Though it could be used directly if we have a few target labels.

Remark Theorem 3.3 shows that if there exists a partition of the feature space such that instances with the same label are within the same component, then aligning the target feature distribution with the reweighted source feature distribution implies *GLS*. While this clustering assumption may seem strong, it is consistent with the goal of reducing classification error: if such a clustering exists, then there also exists a perfect predictor based on the feature $Z = g(X)$, i.e., the cluster index.

We now consider CDAN, an algorithm particularly well-suited for conditional alignment. As described in Section 2, the CDAN discriminator seeks to match $\mathcal{D}_S(\hat{Y} \otimes Z)$ with $\mathcal{D}_T(\hat{Y} \otimes Z)$. This objective is very aligned with *GLS*: let us first assume for argument’s sake that \hat{Y} is a perfect classifier on both domains. For any sample (x, y) , $\hat{y} \otimes z$ is thus a matrix of 0s except on the y -th row, which contains z . When label distributions match, the effect of fooling the discriminator will result in representations such that the matrices $\hat{Y} \otimes Z$ are equal on the source and target domains. In other words, the model is such that $Z \mid Y$ match: it verifies *GLS* (see Th. 3.4 below with $\mathbf{w} = 1$). On the other hand, if the label distributions differ, fooling the discriminator actually requires mislabelling certain samples (a fact quantified in Th. 2.1). We now provide a sufficient condition for *GLS* under a modified CDAN objective (see proofs in App. A.8).

Theorem 3.4. Let $\hat{Y} = h(Z)$, $\gamma := \min_{y \in \mathcal{Y}} \mathcal{D}_T(Y = y)$ and $\mathbf{w}_M := \max_{y \in \mathcal{Y}} \mathbf{w}_y$. For $\tilde{Z} = \hat{Y} \otimes Z$, we have:

$$\max_{y \in \mathcal{Y}} d_{\text{TV}}(\mathcal{D}_S(Z \mid Y = y), \mathcal{D}_T(Z \mid Y = y)) \leq \frac{1}{\gamma} \left(\mathbf{w}_M \varepsilon_S(\hat{Y}) + \varepsilon_T(\hat{Y}) + \sqrt{2D_{\text{JS}}(\mathcal{D}_S^{\mathbf{w}}(\tilde{Z}), \mathcal{D}_T(\tilde{Z}))} \right).$$

Theorem 3.4 suggests that CDANs should match $\mathcal{D}_S^{\mathbf{w}}(\hat{Y} \otimes Z)$ with $\mathcal{D}_T(\hat{Y} \otimes Z)$ to make them robust to mismatched label distributions. In fact, the above upper bound not only applies to CDAN, but also to any algorithm that aims at learning domain-invariant representations⁴.

Theorem 3.5. With the same notations as Th. 3.4:

$$\max_{y \in \mathcal{Y}} d_{\text{TV}}(\mathcal{D}_S(Z \mid Y = y), \mathcal{D}_T(Z \mid Y = y)) \leq \frac{1}{\gamma} \times \left\{ \inf_{\hat{Y}} \left(\mathbf{w}_M \varepsilon_S(\hat{Y}) + \varepsilon_T(\hat{Y}) \right) + \sqrt{8D_{\text{JS}}(\mathcal{D}_S^{\mathbf{w}}(Z), \mathcal{D}_T(Z))} \right\}.$$

Remark . It is worth pointing out that Theorem 3.5 extends Theorem 3.3 by incorporating the clustering assumption as the optimal joint error that is achievable by any classifier based on the representations. In particular, if the clustering structure assumption holds in Theorem 3.3, then the optimal joint error is 0, hence in this case aligning the reweighted feature distributions also implies *GLS*.

3.4 Estimating the Importance Weights \mathbf{w}

Inspired by the moment matching technique to estimate \mathbf{w} under label shift (Lipton et al., 2018), we propose a method to get \mathbf{w} under *GLS* by solving a quadratic program (QP).

Definition 3.5. We let $\mathbf{C} \in \mathbb{R}^{|\mathcal{Y}| \times |\mathcal{Y}|}$ denote the confusion matrix of the classifier on the source domain and $\mu \in \mathbb{R}^{|\mathcal{Y}|}$ the distribution of predictions on the target one, $\forall y, y' \in \mathcal{Y}$:

$$\mathbf{C}_{y,y'} := \mathcal{D}_S(\hat{Y} = y, Y = y'), \quad \mu_y := \mathcal{D}_T(\hat{Y} = y).$$

⁴Th. 3.4 does not stem from Th. 3.5 since the LHS of Th. 3.4 applies to Z , not to \tilde{Z} , and in its RHS, \tilde{Z} depends on \hat{Y} .

The following lemma is adapted from Lipton et al. (2018) to give a consistent estimate of \mathbf{w} under *GLS*; its proof can be found in Appendix A.9.

Lemma 3.2. If *GLS* is verified, and if the confusion matrix \mathbf{C} is invertible, then $\mathbf{w} = \mathbf{C}^{-1}\boldsymbol{\mu}$.

The key insight from Lemma 3.2 is that, in order to estimate the importance vector \mathbf{w} under *GLS*, we do not need access to labels from the target domain. It is however well-known that matrix inversion is numerically unstable, especially with finite sample estimates $\hat{\mathbf{C}}$ and $\hat{\boldsymbol{\mu}}$ of \mathbf{C} and $\boldsymbol{\mu}_y$ ⁵. We propose to solve instead the following QP (written as $QP(\hat{\mathbf{C}}, \hat{\boldsymbol{\mu}})$), whose solution will be consistent if $\hat{\mathbf{C}} \rightarrow \mathbf{C}$ and $\hat{\boldsymbol{\mu}} \rightarrow \boldsymbol{\mu}$:

$$\begin{aligned} & \underset{\mathbf{w}}{\text{minimize}} && \frac{1}{2} \|\hat{\boldsymbol{\mu}} - \hat{\mathbf{C}}\mathbf{w}\|_2^2 \\ & \text{subject to} && \mathbf{w} \geq 0, \mathbf{w}^T \mathcal{D}_S(Y) = 1. \end{aligned} \tag{5}$$

The above QP can be efficiently solved in time $O(|\mathcal{Y}|^3)$, with $|\mathcal{Y}|$ small and constant. Furthermore, by construction, the solution of the above QP is element-wise non-negative, even with limited amounts of data to estimate \mathbf{C} and $\boldsymbol{\mu}_y$.

3.5 \mathcal{F} -IPM for Distributional Alignment

In order to align the target feature distribution and the reweighted source feature distribution as suggested by Lemma 3.1, we now provide a general framework using the integral probability metric (Müller, 1997, IPM).

Definition 3.6. Let \mathcal{F} be a family of real-value functions. The \mathcal{F} -IPM between two distributions \mathcal{D} and \mathcal{D}' is

$$d_{\mathcal{F}}(\mathcal{D}, \mathcal{D}') := \sup_{f \in \mathcal{F}} |\mathbb{E}_{X \sim \mathcal{D}}[f(X)] - \mathbb{E}_{X \sim \mathcal{D}'}[f(X)]|. \tag{6}$$

By approximating any function class \mathcal{F} using parametrized models, e.g., neural networks, we obtain a general framework for domain adaptation by aligning reweighted source feature distribution and target feature distribution, i.e. by minimizing $d_{\mathcal{F}}(\mathcal{D}_T(\tilde{Z}), \mathcal{D}_S^{\mathbf{w}}(\tilde{Z}))$. In particular, by choosing $\mathcal{F} = \{f : \|f\|_{\infty} \leq 1\}$, $d_{\mathcal{F}}$ reduces to total variation and the definition (6) of IPM becomes the negative sum of Type-I and Type-II errors (up to a constant) in distinguishing between \mathcal{D} and \mathcal{D}' . This leads to our first algorithm IWDAN (cf. Section 4.1), an improved variant DANN algorithm that also takes into account the difference between label distributions. Similarly, by instantiating \mathcal{F} to be the set of bounded norm functions in a RKHS \mathcal{H} (Gretton et al., 2012), we obtain maximum mean discrepancy methods, leading to IWJAN (cf. Section 4.1), a variant of JAN (Long et al., 2017) for UDA. Below, we provide a comprehensive empirical evaluation of these variants.

4 Practical Implementation

4.1 Algorithms

In the sections above, we have shown a way to estimate the reweighting vector \mathbf{w} and defined necessary and sufficient conditions on the source and target feature distributions for *GLS* to hold. Together, they suggest simple algorithms based on representation learning: (i) estimate \mathbf{w} on the fly during training, (ii) align the

⁵In fact, $\hat{\mathbf{w}} = \hat{\mathbf{C}}^{-1}\hat{\boldsymbol{\mu}}$ is not even necessarily non-negative.

Algorithm 1 Importance-Weighted Domain Adaptation

```
1: Input: source data  $(x_S, y_S)$ , target data  $x_T$ , representation  $g_\theta$ , classifier  $h_\phi$  and discriminator  $d_\psi$ 
2: Input: epochs  $E$ , batches per epoch  $B$ , batch size  $s$ 
3: Initialize  $\mathbf{w}_1 = 1$ 
4: for  $t = 1$  to  $E$  do
5:   Initialize  $\hat{\mathbf{C}} = 0, \hat{\boldsymbol{\mu}} = 0$ 
6:   for  $b = 1$  to  $B$  do
7:     Sample batches  $(x_S^i, y_S^i)$  and  $(x_T^i)$ 
8:     Maximize  $\mathcal{L}_{DA}^{\mathbf{w}_t}$  w.r.t.  $\theta$ , minimize  $\mathcal{L}_{DA}^{\mathbf{w}_t}$  w.r.t.  $\psi$  and minimize  $\mathcal{L}_C^{\mathbf{w}_t}$  w.r.t.  $\theta$  and  $\phi$ 
9:     for  $i = 1$  to  $s$  do
10:       $\hat{\mathbf{C}}_{\cdot y_S^i} \leftarrow \hat{\mathbf{C}}_{\cdot y_S^i} + h_\phi(g_\theta(x_S^i))$  ( $y_S^i$ -th column)
11:       $\hat{\boldsymbol{\mu}} \leftarrow \hat{\boldsymbol{\mu}} + h_\phi(g_\theta(x_T^i))$ 
12:    end for
13:  end for
14:   $\hat{\mathbf{C}} \leftarrow \hat{\mathbf{C}}/sB$  and  $\hat{\boldsymbol{\mu}} \leftarrow \hat{\boldsymbol{\mu}}/sB$ 
15:   $\mathbf{w}_{t+1} = \lambda QP(\hat{\mathbf{C}}, \hat{\boldsymbol{\mu}}) + (1 - \lambda)\mathbf{w}_t$ 
16: end for
```

feature distributions \tilde{Z} of the target domain with the reweighted feature distribution of the source domain and, (iii) minimize the balanced error rate.

Computing \mathbf{w} requires building estimators $\hat{\mathbf{C}}$ and $\hat{\boldsymbol{\mu}}$ from finite samples of \mathbf{C} and $\boldsymbol{\mu}$. We do so by averaging during each successive epochs the predictions of the classifier on the source and target data. This step corresponds to the inner-most loop of Algorithm 1 (lines 9 to 12) and leads to estimations of $\hat{\mathbf{C}}$ and $\hat{\boldsymbol{\mu}}$. At the end of each epoch, the reweighting vector \mathbf{w} is updated, and the estimators reset to 0. We have found empirically that using an exponential moving average of \mathbf{w} performs better (line 15 in Alg. 1). The results of our experiments all use a factor $\lambda = 0.5$.

With the importance weights \mathbf{w} in hand, we can now define our first algorithm, *Importance-Weighted Domain Adversarial Network* (IWDAN), that seeks to enforce the necessary condition in Lemma 3.1 (*i.e.* to align $\mathcal{D}_S^w(Z)$ and $\mathcal{D}_T(Z)$) using a discriminator. All it requires is to modify the DANN losses \mathcal{L}_{DA} and \mathcal{L}_C . For batches (x_S^i, y_S^i) and (x_T^i) of size s , the weighted domain adaptation loss of IWDAN is:

$$\mathcal{L}_{DA}^{\mathbf{w}}(x_S^i, y_S^i, x_T^i; \theta, \psi) = -\frac{1}{s} \sum_{i=1}^s \mathbf{w}_{y_S^i} \log(d_\psi(g_\theta(x_S^i))) + \log(1 - d_\psi(g_\theta(x_T^i))). \quad (7)$$

We verify in the Appendix, Lemma A.1, that the standard adversarial domain adaptation framework to $\mathcal{L}_{DA}^{\mathbf{w}}$ indeed minimizes the JSD between $\mathcal{D}_S^w(Z)$ and $\mathcal{D}_T(Z)$. Our second algorithm, *Importance-Weighted Joint Adaptation Networks* (IWJAN) is based on JAN (Long et al., 2017) and follows the reweighting principle described in Section 3.5 with \mathcal{F} a learnt RKHS (the exact JAN and IWJAN losses are specified in App.B.4). Finally, our third algorithm, based on CDAN, is *Importance-Weighted Conditional Domain Adversarial Network* (IWCDAN). It follows Th.3.4, which suggests matching $\mathcal{D}_S^w(\hat{Y} \otimes Z)$ with $\mathcal{D}_T(\hat{Y} \otimes Z)$. This can be done by replacing the standard adversarial loss in CDAN with the one on Eq. 7, where d_ψ takes as input $(h_\phi \circ g_\theta) \otimes g_\theta$ instead of g_θ . The classifier loss for our three variants is:

$$\mathcal{L}_C^{\mathbf{w}}(x_S^i, y_S^i; \theta, \phi) = -\frac{1}{s} \sum_{i=1}^s \frac{\mathbf{w}_{y_S^i}}{k\mathcal{D}_S(Y=y)} \log(h_\phi(g_\theta(x_S^i))_{y_S^i}). \quad (8)$$

This reweighting is suggested by our theoretical analysis from Section 3, where we seek to minimize the balanced error rate $\text{BER}_{\mathcal{D}}(\hat{Y} \parallel Y)$. We also define oracle versions, IWDAN-O, IWJAN-O and IWCDAN-O where the weights \mathbf{w} used in the losses are not estimated but computed using the true target label distribution. It gives an idealistic version of the reweighting method, and allows to assess the soundness of *GLS*. IWDAN, IWJAN and IWCDAN correspond to Alg. 1 with their respective loss functions on line 8, the oracle versions simply use the true weights \mathbf{w} instead of \mathbf{w}_t .

4.2 Experiments

We apply our three base algorithms, their importance weighted versions, and the associated oracles to domain adaptation problems from the following datasets: Digits (MNIST \leftrightarrow USPS (LeCun & Cortes, 2010; Dheeru & Karra, 2017)), Visda (2017), Office-31 (Saenko et al., 2010) and Office-Home (Venkateswara et al., 2017)⁶. All values are averages over 5 runs. For full details, see App. B.1 and B.6.

Performance vs D_{JS} First, we artificially generate a family of tasks from MNIST and USPS by considering various random subsets of the classes in either the source or target domain (see Appendix B.5 for details). This results in 100 domain adaptation tasks, with Jensen-Shannon divergences varying between 0 and 0.1. Applying IWDAN and IWCDAN results in Figure 1. We see a clear correlation between the improvements provided by our algorithms and $D_{\text{JS}}(\mathcal{D}_S^Y, \mathcal{D}_T^Y)$, which is well aligned with Theorem 2.1. Moreover, IWDAN outperforms DANN on the 100 tasks and IWCDAN beats CDAN on 94. Even on small divergences, our algorithms do not suffer compared to their base versions.

Original Datasets Average results on each dataset are shown in Table 2 (see Tables in App.B.2 for the per-task breakdown). Our weighted version IWDAN outperforms the basic algorithm DANN by 1.75%, 1.64%, 1.16% and 2.65% on the Digits, Visda, Office-31 and Office-Home tasks respectively. Gains for IWCDAN are more limited, but still present: 0.18%, 0.89%, 0.07% and 1.07% respectively. This can be explained by the fact that, as mentioned above, CDAN already enforces a weak form of *GLS*. Gains for JAN are 0.58%, 0.19% and 0.19%. Beyond mean performance, we show the fraction of times (over all seeds and tasks) our variants outperform the original algorithms⁷. Even if gains are small, our variants provide consistent improvements. Additionally, the oracle versions show larger improvements, which strongly supports enforcing *GLS*.

Subsampled datasets The original datasets have fairly balanced classes, making the JSD between source and target label distributions $D_{\text{JS}}(\mathcal{D}_S^Y \parallel \mathcal{D}_T^Y)$ rather small (Tables 11a, 12a and 13a in the App. B.3). To evaluate our algorithms on larger divergences, we arbitrarily modify the source domains on all the tasks above by considering only 30% of the samples coming from the first half of the classes. This results in much larger divergences (Tables 11b, 12b and 13b). Performance is shown in Table 2 (see Tables in App.B.2 for details). For IWDAN, we see gains of 9.3%, 7.33%, 6.43% and 5.58% on the digits, Visda, Office-31 and Office-Home datasets respectively. For IWCDAN, improvements are 4.99%, 5.64%, 2.26% and 4.99%, and IWJAN shows gains of 6.48%, 4.40% and 1.95%. Moreover, on all seeds and tasks but one, our variants outperform their base versions. Here as well, the oracles perform even better.

⁶Except for JAN, which is not available on Digits.

⁷On the original datasets, the variance between seeds is larger than the difference between algorithms, making it uninformative.

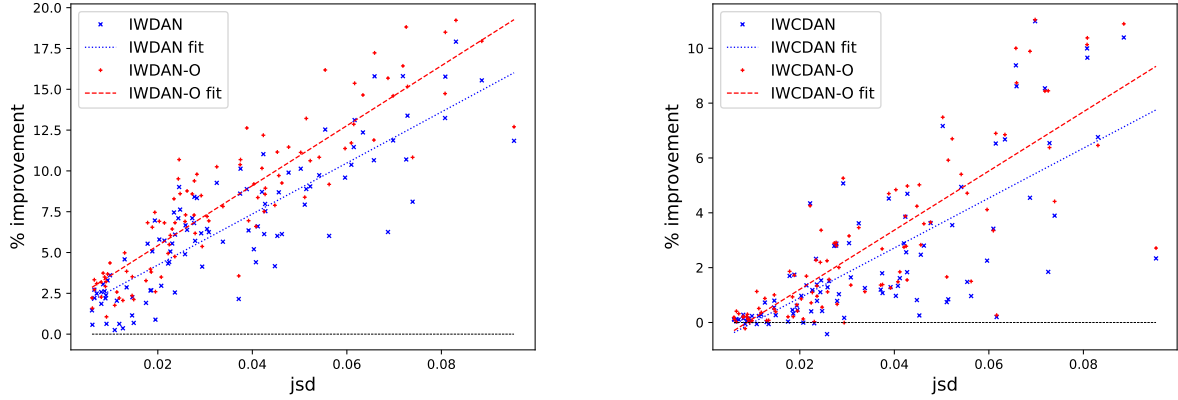


Figure 1: Gains of our algorithms versus their base versions for the 100 tasks described in Section 4 (IWDAN/IWCDAN on the left/right). The x -axis represents $D_{JS}(\mathcal{D}_S^Y, \mathcal{D}_T^Y)$, the JSD between label distributions. Lines represent linear fits. The mean improvements over DANN (resp. CDAN) for IWDAN and IWDAN-O (resp. IWCDAN and IWCDAN-O) are 6.55% and 8.14% (resp. 2.25% and 2.81%).

Ablation Study Our algorithms have two components, a weighted adversarial loss \mathcal{L}_{DA}^w and a weighted classification loss \mathcal{L}_C^w . In Table 3, we augment DANN and CDAN using those losses separately (with the true weights). We observe that DANN benefits essentially from the reweighting of its adversarial loss \mathcal{L}_{DA}^w , the classification loss has little effect. For CDAN, gains are essentially seen on the subsampled datasets. Both losses help, with a +2% extra gain for \mathcal{L}_{DA}^w .

Table 2: Average results on the various domains (Digits has 2 tasks, Visda 1, Office-31 6 and Office-Home 12). The prefix s denotes the experiment where the source domain is subsampled to increase $D_{JS}(\mathcal{D}_S^Y, \mathcal{D}_T^Y)$. Each number is a mean over 5 seeds, the subscript denotes the fraction of times (out of $5 \text{ seeds} \times \#tasks$) our algorithms outperform their base versions.

METHOD	DIGITS	sDIGITS	VISDA	sVISDA	O-31	sO-31	O-H	sO-H
No DA	77.17	75.67	48.39	49.02	77.81	75.72	56.39	51.34
DANN	93.15	83.24	61.88	52.85	82.74	76.17	59.62	51.83
IWDAN	94.90 _{100%}	92.54 _{100%}	63.52 _{100%}	60.18 _{100%}	83.90 _{87%}	82.60 _{100%}	62.27 _{97%}	57.61 _{100%}
IWDAN-O	95.27 _{100%}	94.46 _{100%}	64.19 _{100%}	62.10 _{100%}	85.33 _{97%}	84.41 _{100%}	64.68 _{100%}	60.87 _{100%}
CDAN	95.72	88.23	65.60	60.19	87.23	81.62	64.59	56.25
IWCDAN	95.90 _{80%}	93.22 _{100%}	66.49 _{60%}	65.83 _{100%}	87.30 _{73%}	83.88 _{100%}	65.66 _{70%}	61.24 _{100%}
IWCDAN-O	95.85 _{90%}	94.81 _{100%}	68.15 _{100%}	66.85 _{100%}	88.14 _{90%}	85.47 _{100%}	67.64 _{98%}	63.73 _{100%}
JAN	N/A	N/A	56.98	50.64	85.13	78.21	59.59	53.94
IWJAN	N/A	N/A	57.56 _{100%}	57.12 _{100%}	85.32 _{60%}	82.61 _{97%}	59.78 _{63%}	55.89 _{100%}
IWJAN-O	N/A	N/A	61.48 _{100%}	61.30 _{100%}	87.14 _{100%}	86.24 _{100%}	60.73 _{92%}	57.36 _{100%}

Table 3: Ablation study on the original and subsampled Digits data.

METHOD	DIGITS	SDIGITS
DANN	93.15	83.24
DANN + \mathcal{L}_C^w	93.27	84.52
DANN + \mathcal{L}_{DA}^w	95.31	94.41
IWDAN-O	95.27	94.46
CDAN	95.72	88.23
CDAN + \mathcal{L}_C^w	95.65	91.01
CDAN + \mathcal{L}_{DA}^w	95.42	93.18
IWCDAN-O	95.85	94.81

5 Related Work

Covariate shift has been studied and used in many adaptation algorithms (Huang et al., 2006; Gretton et al., 2009; Ash et al., 2016; Adel et al., 2017; Tzeng et al., 2017; Zhao et al., 2019a; Redko et al., 2019). While less known, label shift has also been tackled from various angles over the years: applying EM to learn \mathcal{D}_T^Y (Chan & Ng, 2005), placing a prior on the label distribution (Storkey, 2009), using kernel mean matching (Zhang et al., 2013; du Plessis & Sugiyama, 2014; Nguyen et al., 2015), etc. Schölkopf et al. (2012) cast the problem in a causal/anti-causal perspective corresponding to covariate/label shift. That perspective was then developed in Zhang et al. (2013); Gong et al. (2016); Lipton et al. (2018); Azizzadenesheli et al. (2019).

Numerous domain adaptation methods rely on learning invariant representations, and minimize various metrics on the marginal feature distributions: total variation or equivalently D_{JS} (Ganin et al., 2016; Tzeng et al., 2017; Zhao et al., 2018b; Liu et al., 2019), maximum mean discrepancy (Gretton et al., 2012; Long et al., 2014, 2015, 2016, 2017), Wasserstein distance (Courty et al., 2017b,a; Shen et al., 2018; Lee & Raginsky, 2018), etc. Other noteworthy DA methods use reconstruction losses and cycle-consistency to learn transferable classifiers (Zhu et al., 2017; Hoffman et al., 2017; Xie et al., 2018). Recently, Liu et al. (2019) have introduced Transferable Adversarial Training (TAT), where transferable examples are generated to fill the gap in feature space between source and target domains, the datasets is then augmented with those samples. The applicability of our method to TAT is a future research direction.

Other relevant settings, avenues for future work, include partial adversarial domain adaptation i.e. UDA when target labels are a strict subset of source labels, or equivalently some components of \mathbf{w} are 0 (Cao et al., 2018a,b, 2019). Multi-domain adaptation, where multiple source or target domains are given, is also very studied (Mansour et al., 2009; Daumé III, 2009; Nam & Han, 2016; Zhao et al., 2018a; Guo et al., 2018; Peng et al., 2019). Recently, Binkowski et al. (2019) study sample reweighting in the domain transfer setting to handle mass shifts between distributions.

6 Discussion and Future Work

We have introduced the generalized label shift assumption and theoretically-grounded variations of existing algorithms to handle mismatched label distributions. On (rather) balanced tasks from classic benchmarks, our algorithms outperform (by small margins) their base versions. On unbalanced datasets, the gain becomes

significant and, as expected theoretically, correlates well with the JSD between label distributions. We now discuss potential improvements.

Improved importance weights estimation All the results above were obtained with $\lambda = 0.5$; we favored simplicity of the algorithm over raw performance. We notice however, that the oracle sometimes shows substantial improvements over the estimated weights algorithm. It suggests that \mathbf{w} is not perfectly estimated and that e.g. fine-tuning λ or updating \mathbf{w} more or less often could lead to better performance. One can also think of settings (e.g. semi-supervised learning) where estimations of \mathcal{D}_T^Y can be obtained via other means.

Extensions The framework we define relies on appropriately reweighting the domain adversarial losses. It can be straightforwardly applied to settings where multiple source and/or target domains are used, by simply maintaining one importance weights vector \mathbf{w} for each source/target pair (Zhao et al., 2018a; Peng et al., 2019). In particular, label shift could explain the observation from Zhao et al. (2018a) that too many source domains sometimes hurt performance, and our framework might alleviate the issue.

References

- Adel, T., Zhao, H., and Wong, A. Unsupervised domain adaptation with a relaxed covariate shift assumption. In *Thirty-First AAAI Conference on Artificial Intelligence*, 2017.
- Arjovsky, M., Bottou, L., Gulrajani, I., and Lopez-Paz, D. Invariant risk minimization, 2019. URL <http://arxiv.org/abs/1907.02893>. cite arxiv:1907.02893.
- Ash, J. T., Schapire, R. E., and Engelhardt, B. E. Unsupervised domain adaptation using approximate label matching. *arXiv preprint arXiv:1602.04889*, 2016.
- Azizzadenesheli, K., Liu, A., Yang, F., and Anandkumar, A. Regularized learning for domain adaptation under label shifts. In *ICLR (Poster)*. OpenReview.net, 2019. URL <http://dblp.uni-trier.de/db/conf/iclr/iclr2019.html#Azizzadenesheli19>.
- Bachman, P., Hjelm, R. D., and Buchwalter, W. Learning representations by maximizing mutual information across views. *CoRR*, abs/1906.00910, 2019. URL <http://dblp.uni-trier.de/db/journals/corr/corr1906.html#abs-1906-00910>.
- Ben-David, S., Blitzer, J., Crammer, K., Pereira, F., et al. Analysis of representations for domain adaptation. *Advances in neural information processing systems*, 19:137, 2007.
- Ben-David, S., Blitzer, J., Crammer, K., Kulesza, A., Pereira, F., and Vaughan, J. W. A theory of learning from different domains. *Machine learning*, 79(1-2):151–175, 2010.
- Binkowski, M., Hjelm, R. D., and Courville, A. C. Batch weight for domain adaptation with mass shift. *CoRR*, abs/1905.12760, 2019. URL <http://dblp.uni-trier.de/db/journals/corr/corr1905.html#abs-1905-12760>.
- Bousmalis, K., Trigeorgis, G., Silberman, N., Krishnan, D., and Erhan, D. Domain separation networks. In *Advances in Neural Information Processing Systems*, pp. 343–351, 2016.
- Briët, J. and Harremoës, P. Properties of classical and quantum jensen-shannon divergence. *Phys. Rev. A*, 79: 052311, May 2009. doi: 10.1103/PhysRevA.79.052311. URL <https://link.aps.org/doi/10.1103/PhysRevA.79.052311>.
- Cao, Z., Long, M., Wang, J., and Jordan, M. I. Partial transfer learning with selective adversarial networks. In *CVPR*, pp. 2724–2732. IEEE Computer Society, 2018a. URL <http://dblp.uni-trier.de/db/conf/cvpr/cvpr2018.html#CaoL0J18>.
- Cao, Z., Ma, L., Long, M., and Wang, J. Partial adversarial domain adaptation. In Ferrari, V., Hebert, M., Sminchisescu, C., and Weiss, Y. (eds.), *ECCV (8)*, volume 11212 of *Lecture Notes in Computer Science*, pp. 139–155. Springer, 2018b. ISBN 978-3-030-01237-3. URL <http://dblp.uni-trier.de/db/conf/eccv/eccv2018-8.html#CaoMLW18>.
- Cao, Z., You, K., Long, M., Wang, J., and Yang, Q. Learning to transfer examples for partial domain adaptation. In *CVPR*, pp. 2985–2994. Computer Vision Foundation / IEEE, 2019. URL <http://dblp.uni-trier.de/db/conf/cvpr/cvpr2019.html#CaoYLW019>.
- Chan, Y. S. and Ng, H. T. Word sense disambiguation with distribution estimation. In Kaelbling, L. P. and Saffiotti, A. (eds.), *IJCAI*, pp. 1010–1015. Professional Book Center, 2005. ISBN 0938075934. URL <http://dblp.uni-trier.de/db/conf/ijcai/ijcai2005.html#ChanN05>.

- Courty, N., Flamary, R., Habrard, A., and Rakotomamonjy, A. Joint distribution optimal transportation for domain adaptation. In *Advances in Neural Information Processing Systems*, pp. 3730–3739, 2017a.
- Courty, N., Flamary, R., Tuia, D., and Rakotomamonjy, A. Optimal transport for domain adaptation. *IEEE transactions on pattern analysis and machine intelligence*, 39(9):1853–1865, 2017b.
- Daumé III, H. Frustratingly easy domain adaptation. *arXiv preprint arXiv:0907.1815*, 2009.
- Dheeru, D. and Karra, E. UCI machine learning repository, 2017. URL <http://archive.ics.uci.edu/ml>.
- du Plessis, M. C. and Sugiyama, M. Semi-supervised learning of class balance under class-prior change by distribution matching. *Neural Networks*, 50:110–119, 2014. URL <http://dblp.uni-trier.de/db/journals/nn/nn50.html#PlessisS14>.
- Endres, D. M. and Schindelin, J. E. A new metric for probability distributions. *IEEE Transactions on Information theory*, 2003.
- Ganin, Y., Ustinova, E., Ajakan, H., Germain, P., Larochelle, H., Laviolette, F., Marchand, M., and Lempitsky, V. Domain-adversarial training of neural networks. *Journal of Machine Learning Research*, 17(59):1–35, 2016.
- Gong, M., Zhang, K., Liu, T., Tao, D., Glymour, C., and Schölkopf, B. Domain adaptation with conditional transferable components. In *International conference on machine learning*, pp. 2839–2848, 2016.
- Goodfellow, I., Bengio, Y., and Courville, A. *Deep learning*. 2017. ISBN 9780262035613 0262035618. URL https://www.worldcat.org/title/deep-learning/oclc/985397543&referer=brief_results.
- Goodfellow, I. J., Pouget-Abadie, J., Mirza, M., Xu, B., Warde-Farley, D., Ozair, S., Courville, A., and Bengio, Y. Generative adversarial networks, 2014. URL <http://arxiv.org/abs/1406.2661>. cite arxiv:1406.2661.
- Gretton, A., Smola, A., Huang, J., Schmittfull, M., Borgwardt, K., and Schölkopf, B. Covariate shift by kernel mean matching. *Dataset shift in machine learning*, 3(4):5, 2009.
- Gretton, A., Borgwardt, K. M., Rasch, M. J., Schölkopf, B., and Smola, A. A kernel two-sample test. *Journal of Machine Learning Research*, 13(Mar):723–773, 2012.
- Guo, J., Shah, D. J., and Barzilay, R. Multi-source domain adaptation with mixture of experts. *arXiv preprint arXiv:1809.02256*, 2018.
- Hoffman, J., Tzeng, E., Park, T., Zhu, J.-Y., Isola, P., Saenko, K., Efros, A. A., and Darrell, T. Cycada: Cycle-consistent adversarial domain adaptation. *arXiv preprint arXiv:1711.03213*, 2017.
- Huang, J., Gretton, A., Borgwardt, K. M., Schölkopf, B., and Smola, A. J. Correcting sample selection bias by unlabeled data. In *Advances in neural information processing systems*, pp. 601–608, 2006.
- LeCun, Y. and Cortes, C. MNIST handwritten digit database. <http://yann.lecun.com/exdb/mnist/>, 2010. URL <http://yann.lecun.com/exdb/mnist/>.

- LeCun, Y., Bottou, L., Bengio, Y., and Haffner, P. Gradient-based learning applied to document recognition. *Proceedings of the IEEE*, 86(11):2278–2324, 1998. ISSN 0018-9219. doi: 10.1109/5.726791.
- Lee, J. and Raginsky, M. Minimax statistical learning with wasserstein distances. In *Advances in Neural Information Processing Systems*, pp. 2692–2701, 2018.
- Lin, J. Divergence measures based on the Shannon entropy. *IEEE Transactions on Information Theory*, 37(1):145–151, 1991.
- Lipton, Z., Wang, Y.-X., and Smola, A. Detecting and correcting for label shift with black box predictors. In *International Conference on Machine Learning*, pp. 3128–3136, 2018.
- Liu, H., Long, M., Wang, J., and Jordan, M. I. Transferable adversarial training: A general approach to adapting deep classifiers. In Chaudhuri, K. and Salakhutdinov, R. (eds.), *ICML*, volume 97 of *Proceedings of Machine Learning Research*, pp. 4013–4022. PMLR, 2019. URL <http://dblp.uni-trier.de/db/conf/icml/icml2019.html#LiuLWJ19>.
- Long, M., Wang, J., Ding, G., Sun, J., and Yu, P. S. Transfer joint matching for unsupervised domain adaptation. In *Proceedings of the IEEE conference on computer vision and pattern recognition*, pp. 1410–1417, 2014.
- Long, M., Cao, Y., Wang, J., and Jordan, M. Learning transferable features with deep adaptation networks. In *International Conference on Machine Learning*, pp. 97–105, 2015.
- Long, M., Zhu, H., Wang, J., and Jordan, M. I. Unsupervised domain adaptation with residual transfer networks. In *Advances in Neural Information Processing Systems*, pp. 136–144, 2016.
- Long, M., Zhu, H., Wang, J., and Jordan, M. I. Deep transfer learning with joint adaptation networks. In *Proceedings of the 34th International Conference on Machine Learning-Volume 70*, pp. 2208–2217. JMLR, 2017.
- Long, M., Cao, Z., Wang, J., and Jordan, M. I. Conditional adversarial domain adaptation. In Bengio, S., Wallach, H. M., Larochelle, H., Grauman, K., Cesa-Bianchi, N., and Garnett, R. (eds.), *NeurIPS*, pp. 1647–1657, 2018. URL <http://dblp.uni-trier.de/db/conf/nips/nips2018.html#LongC0J18>.
- Mansour, Y., Mohri, M., and Rostamizadeh, A. Domain adaptation with multiple sources. In *Advances in neural information processing systems*, pp. 1041–1048, 2009.
- McCoy, R. T., Pavlick, E., and Linzen, T. Right for the wrong reasons: Diagnosing syntactic heuristics in natural language inference. *Proceedings of the ACL*, 2019.
- Müller, A. Integral probability metrics and their generating classes of functions. *Advances in Applied Probability*, 29(2):429–443, 1997.
- Nam, H. and Han, B. Learning multi-domain convolutional neural networks for visual tracking. In *The IEEE Conference on Computer Vision and Pattern Recognition (CVPR)*, June 2016.
- Nguyen, T. D., du Plessis, M. C., and Sugiyama, M. Continuous target shift adaptation in supervised learning. In *ACML*, volume 45 of *JMLR Workshop and Conference Proceedings*, pp. 285–300. JMLR.org, 2015. URL <http://dblp.uni-trier.de/db/conf/acml/acml2015.html#NguyenPS15>.

- Peng, X., Huang, Z., Sun, X., and Saenko, K. Domain agnostic learning with disentangled representations. In Chaudhuri, K. and Salakhutdinov, R. (eds.), *ICML*, volume 97 of *Proceedings of Machine Learning Research*, pp. 5102–5112. PMLR, 2019. URL <http://dblp.uni-trier.de/db/conf/icml/icml2019.html#PengHSS19>.
- Redko, I., Courty, N., Flamary, R., and Tuia, D. Optimal transport for multi-source domain adaptation under target shift. In *22nd International Conference on Artificial Intelligence and Statistics (AISTATS) 2019*, volume 89, 2019.
- Saenko, K., Kulis, B., Fritz, M., and Darrell, T. Adapting visual category models to new domains. In Daniilidis, K., Maragos, P., and Paragios, N. (eds.), *ECCV (4)*, volume 6314 of *Lecture Notes in Computer Science*, pp. 213–226. Springer, 2010. ISBN 978-3-642-15560-4. URL <http://dblp.uni-trier.de/db/conf/eccv/eccv2010-4.html#SaenkoKFD10>.
- Schölkopf, B., Janzing, D., Peters, J., Sgouritsa, E., Zhang, K., and Mooij, J. M. On causal and anticausal learning. In *ICML*. icml.cc / Omnipress, 2012. URL <http://dblp.uni-trier.de/db/conf/icml/icml2012.html#ScholkopfJPSZM12>.
- Shen, J., Qu, Y., Zhang, W., and Yu, Y. Wasserstein distance guided representation learning for domain adaptation. In *Thirty-Second AAAI Conference on Artificial Intelligence*, 2018.
- Storkey, A. When training and test sets are different: Characterising learning transfer. *Dataset shift in machine learning*, 2009.
- Tzeng, E., Hoffman, J., Saenko, K., and Darrell, T. Adversarial discriminative domain adaptation. *arXiv preprint arXiv:1702.05464*, 2017.
- Venkateswara, H., Eusebio, J., Chakraborty, S., and Panchanathan, S. Deep hashing network for unsupervised domain adaptation. In *(IEEE) Conference on Computer Vision and Pattern Recognition (CVPR)*, 2017.
- Visda. Visual domain adaptation challenge, 2017. URL <http://ai.bu.edu/visda-2017/>.
- Xie, S., Zheng, Z., Chen, L., and Chen, C. Learning semantic representations for unsupervised domain adaptation. In Dy, J. G. and Krause, A. (eds.), *ICML*, volume 80 of *Proceedings of Machine Learning Research*, pp. 5419–5428. PMLR, 2018. URL <http://dblp.uni-trier.de/db/conf/icml/icml2018.html#XieZCC18>.
- Yaghoobzadeh, Y., des Combes, R. T., Hazen, T. J., and Sordoni, A. Robust natural language inference models with example forgetting. *CoRR*, abs/1911.03861, 2019. URL <http://dblp.uni-trier.de/db/journals/corr/corr1911.html#abs-1911-03861>.
- Yosinski, J., Clune, J., Bengio, Y., and Lipson, H. How transferable are features in deep neural networks? In *Advances in neural information processing systems*, pp. 3320–3328, 2014.
- Zhang, K., Schölkopf, B., Muandet, K., and Wang, Z. Domain adaptation under target and conditional shift. In *International Conference on Machine Learning*, pp. 819–827, 2013.
- Zhang, X., Yu, F. X., Chang, S.-F., and Wang, S. Deep transfer network: Unsupervised domain adaptation. *CoRR*, abs/1503.00591, 2015. URL <http://dblp.uni-trier.de/db/journals/corr/corr1503.html#ZhangYCW15>.

- Zhao, H., Zhang, S., Wu, G., Gordon, G. J., et al. Multiple source domain adaptation with adversarial learning. In *International Conference on Learning Representations*, 2018a.
- Zhao, H., Zhang, S., Wu, G., Moura, J. M., Costeira, J. P., and Gordon, G. J. Adversarial multiple source domain adaptation. In *Advances in Neural Information Processing Systems*, pp. 8568–8579, 2018b.
- Zhao, H., Hu, J., Zhu, Z., Coates, A., and Gordon, G. Deep generative and discriminative domain adaptation. In *Proceedings of the 18th International Conference on Autonomous Agents and MultiAgent Systems*, pp. 2315–2317. International Foundation for Autonomous Agents and Multiagent Systems, 2019a.
- Zhao, H., Tachet des Combes, R., Zhang, K., and Gordon, G. J. On learning invariant representations for domain adaptation. In Chaudhuri, K. and Salakhutdinov, R. (eds.), *ICML*, volume 97 of *Proceedings of Machine Learning Research*, pp. 7523–7532. PMLR, 2019b. URL <http://dblp.uni-trier.de/db/conf/icml/icml2019.html#0002CZG19>.
- Zhu, J.-Y., Park, T., Isola, P., and Efros, A. A. Unpaired image-to-image translation using cycle-consistent adversarial networks. In *ICCV*, pp. 2242–2251. IEEE Computer Society, 2017. ISBN 978-1-5386-1032-9. URL <http://dblp.uni-trier.de/db/conf/iccv/iccv2017.html#ZhuPIE17>.

A Proofs

In this section, we provide the theoretical material that completes the main text.

A.1 Definition

Definition A.1. Let us recall that for two distributions \mathcal{D} and \mathcal{D}' , the Jensen-Shannon (JSD) divergence $D_{\text{JS}}(\mathcal{D} \parallel \mathcal{D}')$ is defined as:

$$D_{\text{JS}}(\mathcal{D} \parallel \mathcal{D}') := \frac{1}{2}D_{\text{KL}}(\mathcal{D} \parallel \mathcal{D}_M) + \frac{1}{2}D_{\text{KL}}(\mathcal{D}' \parallel \mathcal{D}_M),$$

where $D_{\text{KL}}(\cdot \parallel \cdot)$ is the Kullback–Leibler (KL) divergence and $\mathcal{D}_M := (\mathcal{D} + \mathcal{D}')/2$.

A.2 Consistency of the Weighted Domain Adaptation Loss (7)

For the sake of conciseness, we verify here that the domain adaptation training objective does lead to minimizing the Jensen-Shannon divergence between the weighted feature distribution of the source domain and the feature distribution of the target domain.

Lemma A.1. Let $p(x, y)$ and $q(x)$ be two density distributions, and $w(y)$ be a positive function such that $\int p(y)w(y)dy = 1$. Let $p^w(x) = \int p(x, y)w(y)dy$ denote the w -reweighted marginal distribution of x under p . The minimum value of

$$I(d) := \mathbb{E}_{(x, y) \sim p, x' \sim q}[-w(y) \log(d(x)) - \log(1 - d(x'))]$$

is $\log(4) - 2D_{\text{JS}}(p^w(x) \parallel q(x))$, and is attained for $d^*(x) = \frac{p^w(x)}{p^w(x) + q(x)}$.

Proof. We see that:

$$I(d) = - \iiint [w(y) \log(d(x)) + \log(1 - d(x'))] p(x, y) q(x') dx dx' dy \quad (9)$$

$$= - \int [\int w(y) p(x, y) dy] \log(d(x)) + q(x) \log(1 - d(x)) dx \quad (10)$$

$$= - \int p^w(x) \log(d(x)) + q(x) \log(1 - d(x)) dx. \quad (11)$$

From the last line, we follow the exact method from Goodfellow et al. (2014) to see that point-wise in x the minimum is attained for $d^*(x) = \frac{p^w(x)}{p^w(x) + q(x)}$ and that $I(d^*) = \log(4) - 2D_{\text{JS}}(p^w(x) \parallel q(x))$. ■

Applying Lemma A.1 to $\mathcal{D}_S(Z, Y)$ and $\mathcal{D}_T(Z)$ proves that the domain adaptation objective leads to minimizing $D_{\text{JS}}(\mathcal{D}_S^w(Z) \parallel \mathcal{D}_T(Z))$.

A.3 k -class information-theoretic lower bound

In this section, we prove Theorem 2.1 that extends previous result to the general k -class classification problem.

Theorem 2.1. Suppose that the Markov chain in (1) holds, and that $D_{\text{JS}}(\mathcal{D}_S^Y \parallel \mathcal{D}_T^Y) \geq D_{\text{JS}}(\mathcal{D}_S^{\tilde{Z}} \parallel \mathcal{D}_T^{\tilde{Z}})$, then:

$$\varepsilon_S(h \circ g) + \varepsilon_T(h \circ g) \geq \frac{1}{2} \left(\sqrt{D_{\text{JS}}(\mathcal{D}_S^Y \parallel \mathcal{D}_T^Y)} - \sqrt{D_{\text{JS}}(\mathcal{D}_S^{\tilde{Z}} \parallel \mathcal{D}_T^{\tilde{Z}})} \right)^2.$$

Proof. We essentially follow the proof from Zhao et al. (2019b), except for Lemmas 4.6 that needs to be adapted to the CDAN framework and Lemma 4.7 to k -class classification.

Lemma 4.6 from Zhao et al. (2019b) states that $D_{\text{JS}}(\mathcal{D}_S^{\hat{Y}}, \mathcal{D}_T^{\hat{Y}}) \leq D_{\text{JS}}(\mathcal{D}_S^{\tilde{Z}}, \mathcal{D}_T^{\tilde{Z}})$, which covers the case $\tilde{Z} = Z$.

When $\tilde{Z} = \hat{Y} \otimes Z$, let us first recall that we assume h or equivalently \hat{Y} to be a one-hot prediction of the class. We have the following Markov chain:

$$X \xrightarrow{g} Z \xrightarrow{\tilde{h}} \tilde{Z} \xrightarrow{l} \hat{Y},$$

where $\tilde{h}(z) = h(z) \otimes z$ and $l : \mathcal{Y} \otimes \mathcal{Z} \rightarrow \mathcal{Y}$ returns the index of the non-zero block in $\tilde{h}(z)$. There is only one such block since h is a one-hot, and its index corresponds to the class predicted by h . We can now apply the same proof than in Zhao et al. (2019b) to conclude that:

$$D_{\text{JS}}(\mathcal{D}_S^{\hat{Y}}, \mathcal{D}_T^{\hat{Y}}) \leq D_{\text{JS}}(\mathcal{D}_S^{\tilde{Z}}, \mathcal{D}_T^{\tilde{Z}}). \quad (12)$$

It essentially boils down to a data-processing argument: the discrimination distance between two distributions cannot increase after the same (possibly stochastic) channel (kernel) is applied to both. Here, the channel corresponds to the (potentially randomized) function l .

Remark Additionally, we note that the above inequality holds for *any* \tilde{Z} such that $\hat{Y} = l(\tilde{Z})$ for a (potentially randomized) function l . This covers any and all potential combinations of representations at various layers of the deep net, including the last layer (which corresponds to its predictions \hat{Y}).

Let us move to the second part of the proof. We wish to show that $D_{\text{JS}}(\mathcal{D}^Y, \mathcal{D}^{\hat{Y}}) \leq \varepsilon(h \circ g)$, where \mathcal{D} can be either \mathcal{D}_S or \mathcal{D}_T :

$$\begin{aligned} 2D_{\text{JS}}(\mathcal{D}^Y, \mathcal{D}^{\hat{Y}}) &\leq \|\mathcal{D}^Y - \mathcal{D}^{\hat{Y}}\|_1 && (\text{Lin, 1991}) \\ &= \sum_{i=1}^k |\mathcal{D}(\hat{Y} = i) - \mathcal{D}(Y = i)| \\ &= \sum_{i=1}^k \left| \sum_{j=1}^k \mathcal{D}(\hat{Y} = i | Y = j) \mathcal{D}(Y = j) - \mathcal{D}(Y = i) \right| \\ &= \sum_{i=1}^k |\mathcal{D}(\hat{Y} = i | Y = i) \mathcal{D}(Y = i) - \mathcal{D}(Y = i) + \sum_{j \neq i} \mathcal{D}(\hat{Y} = i | Y = j) \mathcal{D}(Y = j)| \\ &\leq \sum_{i=1}^k |\mathcal{D}(\hat{Y} = i | Y = i) - 1| \mathcal{D}(Y = i) + \sum_{i=1}^k \sum_{j \neq i} \mathcal{D}(\hat{Y} = i | Y = j) \mathcal{D}(Y = j) \\ &= \sum_{i=1}^k \mathcal{D}(\hat{Y} \neq Y | Y = i) \mathcal{D}(Y = i) + \sum_{j=1}^k \sum_{i \neq j} \mathcal{D}(\hat{Y} = i | Y = j) \mathcal{D}(Y = j) \\ &= 2 \sum_{i=1}^k \mathcal{D}(\hat{Y} \neq Y | Y = i) \mathcal{D}(Y = i) = 2\mathcal{D}(\hat{Y} \neq Y) = 2\varepsilon(h \circ g). \end{aligned} \quad (13)$$

We can now apply the triangular inequality to $\sqrt{D_{\text{JS}}}$, which is a distance metric (Endres & Schindelin, 2003),

called the Jensen-Shannon distance. This gives us:

$$\begin{aligned}
\sqrt{D_{\text{JS}}(\mathcal{D}_S^Y, \mathcal{D}_T^Y)} &\leq \sqrt{D_{\text{JS}}(\mathcal{D}_S^Y, \mathcal{D}_S^{\hat{Y}})} + \sqrt{D_{\text{JS}}(\mathcal{D}_S^{\hat{Y}}, \mathcal{D}_T^{\hat{Y}})} + \sqrt{D_{\text{JS}}(\mathcal{D}_T^{\hat{Y}}, \mathcal{D}_T^Y)} \\
&\leq \sqrt{D_{\text{JS}}(\mathcal{D}_S^Y, \mathcal{D}_S^{\hat{Y}})} + \sqrt{D_{\text{JS}}(\mathcal{D}_S^{\hat{Y}}, \mathcal{D}_T^{\hat{Y}})} + \sqrt{D_{\text{JS}}(\mathcal{D}_T^{\hat{Y}}, \mathcal{D}_T^Y)} \\
&\leq \sqrt{\varepsilon_S(h \circ g)} + \sqrt{D_{\text{JS}}(\mathcal{D}_S^{\hat{Y}}, \mathcal{D}_T^{\hat{Y}})} + \sqrt{\varepsilon_T(h \circ g)}.
\end{aligned}$$

where we used Equation (12) for the second inequality and (13) for the third.

Finally, assuming that $D_{\text{JS}}(\mathcal{D}_S^Y, \mathcal{D}_T^Y) \geq D_{\text{JS}}(\mathcal{D}_S^{\hat{Y}}, \mathcal{D}_T^{\hat{Y}})$, we get:

$$\left(\sqrt{D_{\text{JS}}(\mathcal{D}_S^Y, \mathcal{D}_T^Y)} - \sqrt{D_{\text{JS}}(\mathcal{D}_S^{\hat{Y}}, \mathcal{D}_T^{\hat{Y}})} \right)^2 \leq \left(\sqrt{\varepsilon_S(h \circ g)} + \sqrt{\varepsilon_T(h \circ g)} \right)^2 \leq 2(\varepsilon_S(h \circ g) + \varepsilon_T(h \circ g)).$$

which concludes the proof. ■

A.4 Proof of Theorem 3.1

To simplify the notation, we define the error gap $\Delta_\varepsilon(\hat{Y})$ as follows:

$$\Delta_\varepsilon(\hat{Y}) := |\varepsilon_S(\hat{Y}) - \varepsilon_T(\hat{Y})|.$$

Also, in this case we use \mathcal{D}_a , $a \in \{S, T\}$ to mean the source and target distributions respectively. Before we give the proof of Theorem 3.1, we first prove the following two lemmas that will be used in the proof.

Lemma A.2. Define $\gamma_{a,j} := \mathcal{D}_a(Y = j)$, $\forall a \in \{S, T\}, \forall j \in [k]$, then $\forall \alpha_j, \beta_j \geq 0$ such that $\alpha_j + \beta_j = 1$, and $\forall i \neq j$, the following upper bound holds:

$$\begin{aligned}
&|\gamma_{S,j} \mathcal{D}_S(\hat{Y} = i | Y = j) - \gamma_{T,j} \mathcal{D}_T(\hat{Y} = i | Y = j)| \leq \\
&|\gamma_{S,j} - \gamma_{T,j}| \cdot \left(\alpha_j \mathcal{D}_S(\hat{Y} = i | Y = j) + \beta_j \mathcal{D}_T(\hat{Y} = i | Y = j) \right) + \gamma_{S,j} \beta_j \Delta_{\text{CE}}(\hat{Y}) + \gamma_{T,j} \alpha_j \Delta_{\text{CE}}(\hat{Y}).
\end{aligned}$$

Proof. To make the derivation uncluttered, define $\mathcal{D}_j(\hat{Y} = i) := \alpha_j \mathcal{D}_S(\hat{Y} = i | Y = j) + \beta_j \mathcal{D}_T(\hat{Y} = i | Y = j)$ to be the mixture conditional probability of $\hat{Y} = i$ given $Y = j$, where the mixture weight is given by α_j and β_j . Then in order to prove the upper bound in the lemma, it suffices if we give the desired upper bound for the following term

$$\begin{aligned}
&\left| \gamma_{S,j} \mathcal{D}_S(\hat{Y} = i | Y = j) - \gamma_{T,j} \mathcal{D}_T(\hat{Y} = i | Y = j) \right| - |(\gamma_{S,j} - \gamma_{T,j}) \mathcal{D}_j(\hat{Y} = i)| \\
&\leq \left| \left(\gamma_{S,j} \mathcal{D}_S(\hat{Y} = i | Y = j) - \gamma_{T,j} \mathcal{D}_T(\hat{Y} = i | Y = j) \right) - (\gamma_{S,j} - \gamma_{T,j}) \mathcal{D}_j(\hat{Y} = i) \right| \\
&= \left| \gamma_{S,j} (\mathcal{D}_S(\hat{Y} = i | Y = j) - \mathcal{D}_j(\hat{Y} = i)) - \gamma_{T,j} (\mathcal{D}_T(\hat{Y} = i | Y = j) - \mathcal{D}_j(\hat{Y} = i)) \right|,
\end{aligned}$$

following which we will have:

$$\begin{aligned}
&|\gamma_{S,j} \mathcal{D}_S(\hat{Y} = i | Y = j) - \gamma_{T,j} \mathcal{D}_T(\hat{Y} = i | Y = j)| \leq |(\gamma_{S,j} - \gamma_{T,j}) \mathcal{D}_j(\hat{Y} = i)| \\
&+ \left| \gamma_{S,j} (\mathcal{D}_S(\hat{Y} = i | Y = j) - \mathcal{D}_j(\hat{Y} = i)) - \gamma_{T,j} (\mathcal{D}_T(\hat{Y} = i | Y = j) - \mathcal{D}_j(\hat{Y} = i)) \right| \\
&\leq |\gamma_{S,j} - \gamma_{T,j}| \left(\alpha_j \mathcal{D}_S(\hat{Y} = i | Y = j) + \beta_j \mathcal{D}_T(\hat{Y} = i | Y = j) \right) \\
&+ \gamma_{S,j} \left| \mathcal{D}_S(\hat{Y} = i | Y = j) - \mathcal{D}_j(\hat{Y} = i) \right| + \gamma_{T,j} \left| \mathcal{D}_T(\hat{Y} = i | Y = j) - \mathcal{D}_j(\hat{Y} = i) \right|.
\end{aligned}$$

To proceed, let us first simplify $\mathcal{D}_S(\hat{Y} = i \mid Y = j) - \mathcal{D}_j(\hat{Y} = i)$. By definition of $\mathcal{D}_j(\hat{Y} = i) = \alpha_j \mathcal{D}_S(\hat{Y} = i \mid Y = j) + \beta_j \mathcal{D}_T(\hat{Y} = i \mid Y = j)$, we know that:

$$\begin{aligned} & \mathcal{D}_S(\hat{Y} = i \mid Y = j) - \mathcal{D}_j(\hat{Y} = i) \\ &= \mathcal{D}_S(\hat{Y} = i \mid Y = j) - (\alpha_j \mathcal{D}_S(\hat{Y} = i \mid Y = j) + \beta_j \mathcal{D}_T(\hat{Y} = i \mid Y = j)) \\ &= (\mathcal{D}_S(\hat{Y} = i \mid Y = j) - \alpha_j \mathcal{D}_S(\hat{Y} = i \mid Y = j)) - \beta_j \mathcal{D}_T(\hat{Y} = i \mid Y = j) \\ &= \beta_j (\mathcal{D}_S(\hat{Y} = i \mid Y = j) - \mathcal{D}_T(\hat{Y} = i \mid Y = j)). \end{aligned}$$

Similarly, for the second term $\mathcal{D}_T(\hat{Y} = i \mid Y = j) - \mathcal{D}_j(\hat{Y} = i)$, we can show that:

$$\mathcal{D}_T(\hat{Y} = i \mid Y = j) - \mathcal{D}_j(\hat{Y} = i) = \alpha_j (\mathcal{D}_T(\hat{Y} = i \mid Y = j) - \mathcal{D}_S(\hat{Y} = i \mid Y = j)).$$

Plugging these two identities into the above, we can continue the analysis with

$$\begin{aligned} & \left| \gamma_{S,j} (\mathcal{D}_S(\hat{Y} = i \mid Y = j) - \mathcal{D}_j(\hat{Y} = i)) - \gamma_{T,j} (\mathcal{D}_T(\hat{Y} = i \mid Y = j) - \mathcal{D}_j(\hat{Y} = i)) \right| \\ &= \left| \gamma_{S,j} \beta_j (\mathcal{D}_S(\hat{Y} = i \mid Y = j) - \mathcal{D}_T(\hat{Y} = i \mid Y = j)) - \gamma_{T,j} \alpha_j (\mathcal{D}_T(\hat{Y} = i \mid Y = j) - \mathcal{D}_S(\hat{Y} = i \mid Y = j)) \right| \\ &\leq \left| \gamma_{S,j} \beta_j (\mathcal{D}_S(\hat{Y} = i \mid Y = j) - \mathcal{D}_T(\hat{Y} = i \mid Y = j)) \right| + \left| \gamma_{T,j} \alpha_j (\mathcal{D}_T(\hat{Y} = i \mid Y = j) - \mathcal{D}_S(\hat{Y} = i \mid Y = j)) \right| \\ &\leq \gamma_{S,j} \beta_j \Delta_{\text{CE}}(\hat{Y}) + \gamma_{T,j} \alpha_j \Delta_{\text{CE}}(\hat{Y}). \end{aligned}$$

The first inequality holds by the triangle inequality and the second by the definition of the conditional error gap. Combining all the inequalities above completes the proof. \blacksquare

We are now ready to prove the theorem:

Theorem 3.1. (Error Decomposition Theorem) For any classifier $\hat{Y} = (h \circ g)(X)$,

$$|\varepsilon_S(h \circ g) - \varepsilon_T(h \circ g)| \leq \|\mathcal{D}_S^Y - \mathcal{D}_T^Y\|_1 \cdot \text{BER}_{\mathcal{D}_S}(\hat{Y} \parallel Y) + 2(k-1) \Delta_{\text{CE}}(\hat{Y}),$$

where $\|\mathcal{D}_S^Y - \mathcal{D}_T^Y\|_1 := \sum_{i=1}^k |\mathcal{D}_S(Y = i) - \mathcal{D}_T(Y = i)|$ is the L_1 distance between \mathcal{D}_S^Y and \mathcal{D}_T^Y .

Proof of Theorem 3.1. First, by the law of total probability, it is easy to verify that following identity holds for $a \in \{S, T\}$:

$$\mathcal{D}_a(\hat{Y} \neq Y) = \sum_{i \neq j} \mathcal{D}_a(\hat{Y} = i, Y = j) = \sum_{i \neq j} \gamma_{a,j} \mathcal{D}_a(\hat{Y} = i \mid Y = j).$$

Using this identity, to bound the error gap, we have:

$$\begin{aligned} & |\mathcal{D}_S(Y \neq \hat{Y}) - \mathcal{D}_T(Y \neq \hat{Y})| \\ &= \left| \sum_{i \neq j} \gamma_{S,j} \mathcal{D}_S(\hat{Y} = i \mid Y = j) - \sum_{i \neq j} \gamma_{T,j} \mathcal{D}_T(\hat{Y} = i \mid Y = j) \right| \\ &\leq \sum_{i \neq j} |\gamma_{S,j} \mathcal{D}_S(\hat{Y} = i \mid Y = j) - \gamma_{T,j} \mathcal{D}_T(\hat{Y} = i \mid Y = j)|. \end{aligned}$$

Invoking Lemma A.2 to bound the above terms, and since $\forall j \in [k], \gamma_{S,j}, \gamma_{T,j} \in [0, 1], \alpha_j + \beta_j = 1$, we get:

$$\begin{aligned}
& |\mathcal{D}_S(Y \neq \hat{Y}) - \mathcal{D}_T(Y \neq \hat{Y})| \\
& \leq \sum_{i \neq j} |\gamma_{S,j} \mathcal{D}_S(\hat{Y} = i | Y = j) - \gamma_{T,j} \mathcal{D}_T(\hat{Y} = i | Y = j)| \\
& \leq \sum_{i \neq j} |\gamma_{S,j} - \gamma_{T,j}| \cdot \left(\alpha_j \mathcal{D}_S(\hat{Y} = i | Y = j) + \beta_j \mathcal{D}_T(\hat{Y} = i | Y = j) \right) + \gamma_{S,j} \beta_j \Delta_{\text{CE}}(\hat{Y}) + \gamma_{T,j} \alpha_j \Delta_{\text{CE}}(\hat{Y}) \\
& \leq \sum_{i \neq j} |\gamma_{S,j} - \gamma_{T,j}| \cdot \left(\alpha_j \mathcal{D}_S(\hat{Y} = i | Y = j) + \beta_j \mathcal{D}_T(\hat{Y} = i | Y = j) \right) + \gamma_{S,j} \Delta_{\text{CE}}(\hat{Y}) + \gamma_{T,j} \Delta_{\text{CE}}(\hat{Y}) \\
& = \sum_{i \neq j} |\gamma_{S,j} - \gamma_{T,j}| \cdot \left(\alpha_j \mathcal{D}_S(\hat{Y} = i | Y = j) + \beta_j \mathcal{D}_T(\hat{Y} = i | Y = j) \right) + \sum_{i=1}^k \sum_{j \neq i} \gamma_{S,j} \Delta_{\text{CE}}(\hat{Y}) + \gamma_{T,j} \Delta_{\text{CE}}(\hat{Y}) \\
& = \sum_{i \neq j} |\gamma_{S,j} - \gamma_{T,j}| \cdot \left(\alpha_j \mathcal{D}_S(\hat{Y} = i | Y = j) + \beta_j \mathcal{D}_T(\hat{Y} = i | Y = j) \right) + 2(k-1) \Delta_{\text{CE}}(\hat{Y}).
\end{aligned}$$

Note that the above holds $\forall \alpha_j, \beta_j \geq 0$ such that $\alpha_j + \beta_j = 1$. By choosing $\alpha_j = 1, \forall j \in [k]$ and $\beta_j = 0, \forall j \in [k]$, we have:

$$\begin{aligned}
& = \sum_{i \neq j} |\gamma_{S,j} - \gamma_{T,j}| \cdot \mathcal{D}_S(\hat{Y} = i | Y = j) + 2(k-1) \Delta_{\text{CE}}(\hat{Y}) \\
& = \sum_{j=1}^k |\gamma_{S,j} - \gamma_{T,j}| \cdot \left(\sum_{i=1, i \neq j}^k \mathcal{D}_S(\hat{Y} = i | Y = j) \right) + 2(k-1) \Delta_{\text{CE}}(\hat{Y}) \\
& = \sum_{j=1}^k |\gamma_{S,j} - \gamma_{T,j}| \cdot \mathcal{D}_S(\hat{Y} \neq Y | Y = j) + 2(k-1) \Delta_{\text{CE}}(\hat{Y}) \\
& \leq \|\mathcal{D}_S^Y - \mathcal{D}_T^Y\|_1 \cdot \text{BER}_{\mathcal{D}_S}(\hat{Y} \parallel Y) + 2(k-1) \Delta_{\text{CE}}(\hat{Y}),
\end{aligned}$$

where the last line is due to Holder's inequality, completing the proof. \blacksquare

A.5 Proof of Theorem 3.2

Theorem 3.2. If $Z = g(X)$ satisfies GLS, then for any $h : \mathcal{Z} \rightarrow \mathcal{Y}$ and letting $\hat{Y} = h(Z)$ be the predictor, we have $\varepsilon_S(\hat{Y}) + \varepsilon_T(\hat{Y}) \leq 2\text{BER}_{\mathcal{D}_S}(\hat{Y} \parallel Y)$.

Proof. First, by the law of total probability, we have:

$$\begin{aligned}
\varepsilon_S(\hat{Y}) + \varepsilon_T(\hat{Y}) & = \mathcal{D}_S(Y \neq \hat{Y}) + \mathcal{D}_T(Y \neq \hat{Y}) \\
& = \sum_{j=1}^k \sum_{i \neq j} \mathcal{D}_S(\hat{Y} = i | Y = j) \mathcal{D}_S(Y = j) + \mathcal{D}_T(\hat{Y} = i | Y = j) \mathcal{D}_T(Y = j).
\end{aligned}$$

Now, since $\hat{Y} = (h \circ g)(X) = h(Z)$, \hat{Y} is a function of Z . Given the generalized label shift assumption, this guarantees that:

$$\forall y, y' \in \mathcal{Y}, \quad \mathcal{D}_S(\hat{Y} = y' \mid Y = y) = \mathcal{D}_T(\hat{Y} = y' \mid Y = y).$$

Thus:

$$\begin{aligned} \varepsilon_S(\hat{Y}) + \varepsilon_T(\hat{Y}) &= \sum_{j=1}^k \sum_{i \neq j} \mathcal{D}_S(\hat{Y} = i \mid Y = j) (\mathcal{D}_S(Y = j) + \mathcal{D}_T(Y = j)) \\ &= \sum_{j \in [k]} \mathcal{D}_S(\hat{Y} \neq Y \mid Y = j) \cdot (\mathcal{D}_S(Y = j) + \mathcal{D}_T(Y = j)) \\ &\leq \max_{j \in [k]} \mathcal{D}_S(\hat{Y} \neq Y \mid Y = j) \cdot \sum_{j \in [k]} \mathcal{D}_S(Y = j) + \mathcal{D}_T(Y = j) \\ &= 2\text{BER}_{\mathcal{D}_S}(\hat{Y} \parallel Y). \end{aligned} \quad \blacksquare$$

A.6 Proof of Lemma 3.1

Lemma 3.1. Assuming $Z = g(X)$ satisfies GLS, then $\mathcal{D}_T(Z) = \sum_{y \in \mathcal{Y}} \mathbf{w}_y \cdot \mathcal{D}_S(Z, Y = y) =: \mathcal{D}_S^{\mathbf{w}}(Z)$.

Proof. Using (2) and (4) on the second line:

$$\begin{aligned} \mathcal{D}_T(Z) &= \sum_{y \in \mathcal{Y}} \mathcal{D}_T(Y = y) \cdot \mathcal{D}_T(Z \mid Y = y) \\ &= \sum_{y \in \mathcal{Y}} \mathbf{w}_y \cdot \mathcal{D}_S(Y = y) \cdot \mathcal{D}_S(Z \mid Y = y) \\ &= \sum_{y \in \mathcal{Y}} \mathbf{w}_y \cdot \mathcal{D}_S(Z, Y = y). \end{aligned} \quad \blacksquare$$

A.7 Proof of Theorem 3.3

Theorem 3.3. (Clustering structure implies sufficiency) Let $Z = g(X)$ such that $\mathcal{D}_T(Z) = \mathcal{D}_S^{\mathbf{w}}(Z)$. Assume $\mathcal{D}_T(Y = y) > 0, \forall y \in \mathcal{Y}$. If there exists a partition of $\mathcal{Z} = \cup_{y \in \mathcal{Y}} \mathcal{Z}_y$ such that $\forall y \in \mathcal{Y}$, $\mathcal{D}_S(Z \in \mathcal{Z}_y \mid Y = y) = \mathcal{D}_T(Z \in \mathcal{Z}_y \mid Y = y) = 1$, then $Z = g(X)$ satisfies GLS.

Proof. Follow the condition that $\mathcal{D}_T(Z) = \mathcal{D}_S^{\mathbf{w}}(Z)$, by definition of $\mathcal{D}_S^{\mathbf{w}}(Z)$, we have:

$$\begin{aligned} \mathcal{D}_T(Z) &= \sum_{y \in \mathcal{Y}} \frac{\mathcal{D}_T(Y = y)}{\mathcal{D}_S(Y = y)} \mathcal{D}_S(Z, Y = y) \iff \mathcal{D}_T(Z) = \sum_{y \in \mathcal{Y}} \mathcal{D}_T(Y = y) \mathcal{D}_S(Z \mid Y = y) \\ &\iff \sum_{y \in \mathcal{Y}} \mathcal{D}_T(Y = y) \mathcal{D}_T(Z \mid Y = y) = \sum_{y \in \mathcal{Y}} \mathcal{D}_T(Y = y) \mathcal{D}_S(Z \mid Y = y). \end{aligned}$$

Note that the above equation holds for all measurable subsets of \mathcal{Z} . Now by the assumption that $\mathcal{Z} = \cup_{y \in \mathcal{Y}} \mathcal{Z}_y$ is a partition of \mathcal{Z} , consider $\mathcal{Z}_{y'}$:

$$\sum_{y \in \mathcal{Y}} \mathcal{D}_T(Y = y) \mathcal{D}_T(Z \in \mathcal{Z}_{y'} \mid Y = y) = \sum_{y \in \mathcal{Y}} \mathcal{D}_T(Y = y) \mathcal{D}_S(Z \in \mathcal{Z}_{y'} \mid Y = y).$$

Due to the assumption $\mathcal{D}_S(Z \in \mathcal{Z}_y \mid Y = y) = \mathcal{D}_T(Z \in \mathcal{Z}_y \mid Y = y) = 1$, we know that $\forall y' \neq y$, $\mathcal{D}_T(Z \in \mathcal{Z}_{y'} \mid Y = y) = \mathcal{D}_S(Z \in \mathcal{Z}_{y'} \mid Y = y) = 0$. This shows that both the supports of $\mathcal{D}_S(Z \mid Y = y)$

and $\mathcal{D}_T(Z \mid Y = y)$ are contained in \mathcal{Z}_y . Now consider an arbitrary measurable set $E \subseteq \mathcal{Z}_y$, since $\cup_{y \in \mathcal{Y}} \mathcal{Z}_y$ is a partition of \mathcal{Z} , we know that

$$\mathcal{D}_S(Z \in E \mid Y = y') = \mathcal{D}_T(Z \in E \mid Y = y') = 0, \quad \forall y' \neq y.$$

Plug $Z \in E$ into the following identity:

$$\begin{aligned} \sum_{y \in \mathcal{Y}} \mathcal{D}_T(Y = y) \mathcal{D}_T(Z \in E \mid Y = y) &= \sum_{y \in \mathcal{Y}} \mathcal{D}_T(Y = y) \mathcal{D}_S(Z \in E \mid Y = y) \\ \implies \mathcal{D}_T(Y = y) \mathcal{D}_T(Z \in E \mid Y = y) &= \mathcal{D}_T(Y = y) \mathcal{D}_S(Z \in E \mid Y = y) \\ \implies \mathcal{D}_T(Z \in E \mid Y = y) &= \mathcal{D}_S(Z \in E \mid Y = y), \end{aligned}$$

where the last line holds because $\mathcal{D}_T(Y = y) \neq 0$. Realize that the choice of E is arbitrary, this shows that $\mathcal{D}_S(Z \mid Y = y) = \mathcal{D}_T(Z \mid Y = y)$, which completes the proof. \blacksquare

A.8 Sufficient Conditions for GLS

Theorem 3.4. Let $\hat{Y} = h(Z)$, $\gamma := \min_{y \in \mathcal{Y}} \mathcal{D}_T(Y = y)$ and $\mathbf{w}_M := \max_{y \in \mathcal{Y}} \mathbf{w}_y$. For $\tilde{Z} = \hat{Y} \otimes Z$, we have:

$$\begin{aligned} \max_{y \in \mathcal{Y}} d_{\text{TV}}(\mathcal{D}_S(Z \mid Y = y), \mathcal{D}_T(Z \mid Y = y)) &\leq \\ &\frac{1}{\gamma} \left(\mathbf{w}_M \varepsilon_S(\hat{Y}) + \varepsilon_T(\hat{Y}) + \sqrt{2D_{\text{JS}}(\mathcal{D}_S^{\mathbf{w}}(\tilde{Z}), \mathcal{D}_T(\tilde{Z}))} \right). \end{aligned}$$

Proof. For a given class y , we let R_y denote the y -th row of $\hat{Y} \otimes Z$. R_y is a random variable that lives in \mathcal{Z} . Let us consider a measurable set $E \subseteq \mathcal{Z}$. Two options exist:

- $\mathbf{0} \in E$, in which case: $\{R_y \in E\} = (\{Z \in E\} \cap \{\hat{Y} = y\}) \cup \{\hat{Y} \neq y\}$,
- $\mathbf{0} \notin E$, in which case: $\{R_y \in E\} = \{Z \in E\} \cap \{\hat{Y} = y\}$.

This allows us to write:

$$\begin{aligned} \mathcal{D}_S^{\mathbf{w}}(R_y \in E) &= \mathcal{D}_S^{\mathbf{w}}(Z \in E, \hat{Y} = y) + \mathbb{1}_{\{\mathbf{0} \in E\}} \mathcal{D}_S^{\mathbf{w}}(\hat{Y} \neq y) \\ &= \sum_{y'} \mathcal{D}_S(Z \in E, \hat{Y} = y, Y = y') \mathbf{w}_{y'} + \mathbb{1}_{\{\mathbf{0} \in E\}} \sum_{y', y'' \neq y} \mathcal{D}_S(\hat{Y} = y'', Y = y') \mathbf{w}_{y'} \end{aligned} \tag{14}$$

$$\begin{aligned} \mathcal{D}_T(R_y \in E) &= \mathcal{D}_T(Z \in E, \hat{Y} = y) + \mathbb{1}_{\{\mathbf{0} \in E\}} \mathcal{D}_T(\hat{Y} \neq y) \\ &= \sum_{y'} \mathcal{D}_T(Z \in E, \hat{Y} = y, Y = y') + \mathbb{1}_{\{\mathbf{0} \in E\}} \sum_{y', y'' \neq y} \mathcal{D}_T(\hat{Y} = y'', Y = y'). \end{aligned} \tag{15}$$

We are interested in the quantity

$$|\mathcal{D}_S(Z \in E \mid Y = y) - \mathcal{D}_T(Z \in E \mid Y = y)| = \frac{1}{\mathcal{D}_T(Y = y)} |\mathcal{D}_S(Z \in E, Y = y) \mathbf{w}_y - \mathcal{D}_T(Z \in E, Y = y)|,$$

which we bound below:

$$\begin{aligned}
& |\mathcal{D}_S(Z \in E, Y = y)\mathbf{w}_y - \mathcal{D}_T(Z \in E, Y = y)| \\
&= |\mathcal{D}_S(Z \in E, Y = y)\mathbf{w}_y - \mathcal{D}_S^\mathbf{w}(R_y \in E) + \mathcal{D}_S^\mathbf{w}(R_y \in E) - \mathcal{D}_T(R_y \in E) \\
&\quad + \mathcal{D}_T(R_y \in E) - \mathcal{D}_T(Z \in E, Y = y)| \\
&= |\mathcal{D}_S(Z \in E, Y = y)\mathbf{w}_y - \mathcal{D}_S^\mathbf{w}(Z \in E, \hat{Y} = y) - \mathbb{1}_{\{\mathbf{0} \in E\}} \mathcal{D}_S^\mathbf{w}(\hat{Y} \neq y) + \mathcal{D}_S^\mathbf{w}(R_y \in E) - \mathcal{D}_T(R_y \in E) \\
&\quad + \mathbb{1}_{\{\mathbf{0} \in E\}} \mathcal{D}_T(\hat{Y} \neq y) + \mathcal{D}_T(Z \in E, \hat{Y} = y) - \mathcal{D}_T(Z \in E, Y = y)| \\
&\leq |\mathcal{D}_S(Z \in E, Y = y)\mathbf{w}_y - \mathcal{D}_S^\mathbf{w}(Z \in E, \hat{Y} = y)| + \mathbb{1}_{\{\mathbf{0} \in E\}} |\mathcal{D}_S^\mathbf{w}(\hat{Y} \neq y) - \mathcal{D}_T(\hat{Y} \neq y)| \\
&\quad + |\mathcal{D}_S^\mathbf{w}(R_y \in E) - \mathcal{D}_T(R_y \in E)| + |\mathcal{D}_T(Z \in E, \hat{Y} = y) - \mathcal{D}_T(Z \in E, Y = y)| \\
&\leq |\mathcal{D}_S(Z \in E, Y = y)\mathbf{w}_y - \mathcal{D}_S^\mathbf{w}(Z \in E, \hat{Y} = y)| + |\mathcal{D}_S^\mathbf{w}(\hat{Y} \neq y) - \mathcal{D}_T(\hat{Y} \neq y)| \\
&\quad + D_{TV}(\mathcal{D}_S^\mathbf{w}(R_y), \mathcal{D}_T(R_y)) + |\mathcal{D}_T(Z \in E, \hat{Y} = y) - \mathcal{D}_T(Z \in E, Y = y)|, \tag{16}
\end{aligned}$$

where we used Eqs.14 and 15 on the third line, the triangle inequality on the fourth and $\sup_E |\mathcal{D}_S^\mathbf{w}(R_y \in E) - \mathcal{D}_T(R_y \in E)| = D_{TV}(\mathcal{D}_S^\mathbf{w}(R_y), \mathcal{D}_T(R_y))$ on the last. Let us start by upper-bounding the first term:

$$\begin{aligned}
& |\mathcal{D}_S(Z \in E, Y = y)\mathbf{w}_y - \mathcal{D}_S^\mathbf{w}(Z \in E, \hat{Y} = y)| \\
&= \left| \sum_{y'} \mathcal{D}_S(Z \in E, \hat{Y} = y, Y = y')\mathbf{w}_{y'} - \sum_{y'} \mathcal{D}_S(Z \in E, \hat{Y} = y', Y = y)\mathbf{w}_y \right| \\
&\leq \left| \sum_{y' \neq y} \mathcal{D}_S(Z \in E, \hat{Y} = y, Y = y')\mathbf{w}_{y'} - \mathcal{D}_S(Z \in E, \hat{Y} = y', Y = y)\mathbf{w}_y \right| \\
&\leq \mathbf{w}_M \sum_{y' \neq y} \mathcal{D}_S(Z \in E, \hat{Y} = y, Y = y') + \mathcal{D}_S(Z \in E, \hat{Y} = y', Y = y) \\
&\leq \mathbf{w}_M \mathcal{D}_S(Z \in E, \hat{Y} \neq Y) \leq \mathbf{w}_M \varepsilon_S(\hat{Y}).
\end{aligned}$$

Similarly, we can prove that: $|\mathcal{D}_T(R_y \in E) - \mathcal{D}_T(Z \in E, Y = y)| \leq \varepsilon_T(\hat{Y})$ which bounds the third term of 16. As far as the second term is concerned:

$$\begin{aligned}
& |\mathcal{D}_S^\mathbf{w}(\hat{Y} \neq y) - \mathcal{D}_T(\hat{Y} \neq y)| = \left| \sum_{y', y'' \neq y} \mathcal{D}_S(\hat{Y} = y'', Y = y')\mathbf{w}_{y'} - \sum_{y', y'' \neq y} \mathcal{D}_T(\hat{Y} = y'', Y = y') \right| \\
&\leq \left| \sum_{y'} \mathcal{D}_S(Y = y')\mathbf{w}_{y'} - \sum_{y'} \mathcal{D}_T(Y = y') \right| \\
&\quad + \left| \sum_{y' \neq y} \mathcal{D}_S(\hat{Y} = y, Y = y')\mathbf{w}_{y'} - \sum_{y' \neq y} \mathcal{D}_T(\hat{Y} = y, Y = y') \right. \\
&\quad \left. + \mathcal{D}_S(\hat{Y} = y, Y = y)\mathbf{w}_y - \mathcal{D}_T(\hat{Y} = y, Y = y) \right| \\
&\leq \left| \sum_{y' \neq y} \mathcal{D}_S(\hat{Y} = y, Y = y')\mathbf{w}_{y'} - \sum_{y' \neq y} \mathcal{D}_T(\hat{Y} = y, Y = y') \right. \\
&\quad \left. + \mathcal{D}_S(Y = y)\mathbf{w}_y - \mathcal{D}_S(\hat{Y} \neq y, Y = y)\mathbf{w}_y \right. \\
&\quad \left. - \mathcal{D}_T(Y = y) + \mathcal{D}_T(\hat{Y} \neq y, Y = y) \right| \\
&\leq \sum_{y' \neq y} \mathcal{D}_S(\hat{Y} = y, Y = y')\mathbf{w}_{y'} + \mathcal{D}_S(\hat{Y} \neq y, Y = y)\mathbf{w}_y \\
&\quad + \sum_{y' \neq y} \mathcal{D}_T(\hat{Y} = y, Y = y') + \mathcal{D}_T(\hat{Y} \neq y, Y = y) \\
&\leq \mathbf{w}_M \varepsilon_S(\hat{Y}) + \varepsilon_T(\hat{Y})
\end{aligned}$$

where the first term of the first inequality disappeared because $\forall y' \in \mathcal{Y}, \mathcal{D}_S(Y = y')\mathbf{w}_{y'} = \mathcal{D}_T(Y = y')$ (we also used that property in the second line of the second inequality). Combining these in Eq.16, this guarantees that for any measurable set E :

$$|\mathcal{D}_S(Z \in E, Y = y)\mathbf{w}_y - \mathcal{D}_T(Z \in E, Y = y)| \leq 2\mathbf{w}_{M\mathcal{E}_S(\hat{Y})} + D_{TV}(\mathcal{D}_S^{\mathbf{w}}(R_y), \mathcal{D}_T(R_y)) + 2\varepsilon_T(\hat{Y}).$$

Finally, we have $D_{TV}(\mathcal{D}_S^{\mathbf{w}}(R_y), \mathcal{D}_T(R_y)) \leq D_{TV}(\mathcal{D}_S^{\mathbf{w}}(\hat{Y} \otimes Z) \parallel \mathcal{D}_T(\hat{Y} \otimes Z))$ and from Briët & Harremoës (2009), $D_{TV}(\mathcal{D}_S^{\mathbf{w}}(\hat{Y} \otimes Z) \parallel \mathcal{D}_T(\hat{Y} \otimes Z)) \leq \sqrt{8D_{JS}(\mathcal{D}_S^{\mathbf{w}}(\hat{Y} \otimes Z) \parallel \mathcal{D}_T(\hat{Y} \otimes Z))}$ (the total variation and Jensen-Shannon distance are equivalent), which gives us straightforwardly:

$$\begin{aligned} |\mathcal{D}_S(Z \in E \mid Y = y) - \mathcal{D}_T(Z \in E \mid Y = y)| &= \frac{1}{\mathcal{D}_T(Y = y)} |\mathcal{D}_S(Z \in E, Y = y)\mathbf{w}_y - \mathcal{D}_T(Z \in E, Y = y)| \\ &\leq \frac{1}{\mathcal{D}_T(Y = y)} \left(2\mathbf{w}_{M\mathcal{E}_S(\hat{Y})} + D_{TV}(\mathcal{D}_S^{\mathbf{w}}(R_y), \mathcal{D}_T(R_y)) + 2\varepsilon_T(\hat{Y}) \right) \\ &\leq \frac{1}{\mathcal{D}_T(Y = y)} \left(2\mathbf{w}_{M\mathcal{E}_S(\hat{Y})} + \sqrt{8D_{JS}(\mathcal{D}_S^{\mathbf{w}}(\tilde{Z}) \parallel \mathcal{D}_T(\tilde{Z}))} + 2\varepsilon_T(\hat{Y}) \right). \end{aligned}$$

Using the fact that $D_{TV}(\mathcal{D}_S(Z \mid Y = y), \mathcal{D}_T(Z \mid Y = y)) = \sup_E |\mathcal{D}_S(Z \in E \mid Y = y) - \mathcal{D}_T(Z \in E \mid Y = y)|$ gives:

$$\begin{aligned} D_{TV}(\mathcal{D}_S(Z \mid Y = y), \mathcal{D}_T(Z \mid Y = y)) &\leq \frac{2}{\mathcal{D}_T(Y = y)} \left(\mathbf{w}_{M\mathcal{E}_S(\hat{Y})} + \sqrt{2D_{JS}(\mathcal{D}_S^{\mathbf{w}}(\tilde{Z}) \parallel \mathcal{D}_T(\tilde{Z}))} + \varepsilon_T(\hat{Y}) \right) \\ &\leq \frac{2}{\gamma} \left(\mathbf{w}_{M\mathcal{E}_S(\hat{Y})} + \sqrt{2D_{JS}(\mathcal{D}_S^{\mathbf{w}}(\tilde{Z}) \parallel \mathcal{D}_T(\tilde{Z}))} + \varepsilon_T(\hat{Y}) \right). \end{aligned}$$

Taking the maximum over y on the left-hand side concludes the proof. ■

Theorem 3.5. With the same notations as Th. 3.4:

$$\begin{aligned} \max_{y \in \mathcal{Y}} d_{TV}(\mathcal{D}_S(Z \mid Y = y), \mathcal{D}_T(Z \mid Y = y)) &\leq \\ &\frac{1}{\gamma} \times \left\{ \inf_{\hat{Y}} \left(\mathbf{w}_{M\mathcal{E}_S(\hat{Y})} + \varepsilon_T(\hat{Y}) \right) + \sqrt{8D_{JS}(\mathcal{D}_S^{\mathbf{w}}(Z), \mathcal{D}_T(Z))} \right\}. \end{aligned}$$

Proof. To prove the above upper bound, let us first fix a $y \in \mathcal{Y}$ and fix a classifier $\hat{Y} = h(Z)$ for some $h : \mathcal{Z} \rightarrow \mathcal{Y}$. Now consider any measurable subset $E \subseteq \mathcal{Z}$, we would like to upper bound the following quantity:

$$\begin{aligned} |\mathcal{D}_S(Z \in E \mid Y = y) - \mathcal{D}_T(Z \in E \mid Y = y)| &= \frac{1}{\mathcal{D}_T(Y = y)} \cdot |\mathcal{D}_S(Z \in E, Y = y)\mathbf{w}_y - \mathcal{D}_T(Z \in E, Y = y)| \\ &\leq \frac{1}{\gamma} \cdot |\mathcal{D}_S(Z \in E, Y = y)\mathbf{w}_y - \mathcal{D}_T(Z \in E, Y = y)|. \end{aligned}$$

Hence it suffices if we can upper bound $|\mathcal{D}_S(Z \in E, Y = y)\mathbf{w}_y - \mathcal{D}_T(Z \in E, Y = y)|$. To do so, consider

the following decomposition:

$$\begin{aligned}
|\mathcal{D}_T(Z \in E, Y = y) - \mathcal{D}_S(Z \in E, Y = y)\mathbf{w}_y| &= |\mathcal{D}_T(Z \in E, Y = y) - \mathcal{D}_T(Z \in E, \hat{Y} = y) \\
&\quad + \mathcal{D}_T(Z \in E, \hat{Y} = y) - \mathcal{D}_S^\mathbf{w}(Z \in E, \hat{Y} = y) \\
&\quad + \mathcal{D}_S^\mathbf{w}(Z \in E, \hat{Y} = y) - \mathcal{D}_S(Z \in E, Y = y)\mathbf{w}_y| \\
&\leq |\mathcal{D}_T(Z \in E, Y = y) - \mathcal{D}_T(Z \in E, \hat{Y} = y)| \\
&\quad + |\mathcal{D}_T(Z \in E, \hat{Y} = y) - \mathcal{D}_S^\mathbf{w}(Z \in E, \hat{Y} = y)| \\
&\quad + |\mathcal{D}_S^\mathbf{w}(Z \in E, \hat{Y} = y) - \mathcal{D}_S(Z \in E, Y = y)\mathbf{w}_y|.
\end{aligned}$$

We bound the above three terms in turn. First, consider $|\mathcal{D}_T(Z \in E, Y = y) - \mathcal{D}_T(Z \in E, \hat{Y} = y)|$:

$$\begin{aligned}
|\mathcal{D}_T(Z \in E, Y = y) - \mathcal{D}_T(Z \in E, \hat{Y} = y)| &= \left| \sum_{y'} \mathcal{D}_T(Z \in E, Y = y, \hat{Y} = y') - \sum_{y'} \mathcal{D}_T(Z \in E, \hat{Y} = y, Y = y') \right| \\
&\leq \sum_{y' \neq y} |\mathcal{D}_T(Z \in E, Y = y, \hat{Y} = y') - \mathcal{D}_T(Z \in E, \hat{Y} = y, Y = y')| \\
&\leq \sum_{y' \neq y} \mathcal{D}_T(Z \in E, Y = y, \hat{Y} = y') + \mathcal{D}_T(Z \in E, \hat{Y} = y, Y = y') \\
&\leq \sum_{y' \neq y} \mathcal{D}_T(Y = y, \hat{Y} = y') + \mathcal{D}_T(\hat{Y} = y, Y = y') \\
&\leq \mathcal{D}_T(Y \neq \hat{Y}) \\
&= \varepsilon_T(\hat{Y}),
\end{aligned}$$

where the last inequality is due to the fact that the definition of error rate corresponds to the sum of all the off-diagonal elements in the confusion matrix while the sum here only corresponds to the sum of all the elements in two slices. Similarly, we can bound the third term as follows:

$$\begin{aligned}
|\mathcal{D}_S^\mathbf{w}(Z \in E, \hat{Y} = y) - \mathcal{D}_S(Z \in E, Y = y)\mathbf{w}_y| &= \left| \sum_{y'} \mathcal{D}_S(Z \in E, \hat{Y} = y, Y = y')\mathbf{w}_{y'} - \sum_{y'} \mathcal{D}_S(Z \in E, \hat{Y} = y', Y = y)\mathbf{w}_y \right| \\
&\leq \left| \sum_{y' \neq y} \mathcal{D}_S(Z \in E, \hat{Y} = y, Y = y')\mathbf{w}_{y'} - \mathcal{D}_S(Z \in E, \hat{Y} = y', Y = y)\mathbf{w}_y \right| \\
&\leq \mathbf{w}_M \sum_{y' \neq y} \mathcal{D}_S(Z \in E, \hat{Y} = y, Y = y') + \mathcal{D}_S(Z \in E, \hat{Y} = y', Y = y) \\
&\leq \mathbf{w}_M \mathcal{D}_S(Z \in E, \hat{Y} \neq Y) \\
&\leq \mathbf{w}_M \varepsilon_S(\hat{Y}).
\end{aligned}$$

Now we bound the last term. Recall the definition of total variation, we have:

$$\begin{aligned}
|\mathcal{D}_T(Z \in E, \hat{Y} = y) - \mathcal{D}_S^\mathbf{w}(Z \in E, \hat{Y} = y)| &= |\mathcal{D}_T(Z \in E \wedge Z \in \hat{Y}^{-1}(y)) - \mathcal{D}_S^\mathbf{w}(Z \in E \wedge Z \in \hat{Y}^{-1}(y))| \\
&\leq \sup_{E' \text{ is measurable}} |\mathcal{D}_T(Z \in E') - \mathcal{D}_S^\mathbf{w}(Z \in E')| \\
&= d_{\text{TV}}(\mathcal{D}_T(Z), \mathcal{D}_S^\mathbf{w}(Z)).
\end{aligned}$$

Combining the above three parts yields

$$|\mathcal{D}_S(Z \in E \mid Y = y) - \mathcal{D}_T(Z \in E \mid Y = y)| \leq \frac{1}{\gamma} \cdot \left(\mathbf{w}_{M\mathcal{E}_S}(\hat{Y}) + \varepsilon_T(\hat{Y}) + d_{\text{TV}}(\mathcal{D}_S^{\mathbf{w}}(Z), \mathcal{D}_T(Z)) \right).$$

Now realizing that the choice of $y \in \mathcal{Y}$ and the measurable subset E on the LHS is arbitrary, this leads to

$$\max_{y \in \mathcal{Y}} \sup_E |\mathcal{D}_S(Z \in E \mid Y = y) - \mathcal{D}_T(Z \in E \mid Y = y)| \leq \frac{1}{\gamma} \cdot \left(\mathbf{w}_{M\mathcal{E}_S}(\hat{Y}) + \varepsilon_T(\hat{Y}) + d_{\text{TV}}(\mathcal{D}_S^{\mathbf{w}}(Z), \mathcal{D}_T(Z)) \right).$$

Furthermore, notice that the above upper bound holds for any classifier $\hat{Y} = h(Z)$, hence we have

$$\max_{y \in \mathcal{Y}} d_{\text{TV}}(\mathcal{D}_S(Z \in E \mid Y = y), \mathcal{D}_T(Z \in E \mid Y = y)) \leq \frac{1}{\gamma} \cdot \inf_{\hat{Y}} \left(\mathbf{w}_{M\mathcal{E}_S}(\hat{Y}) + \varepsilon_T(\hat{Y}) + d_{\text{TV}}(\mathcal{D}_S^{\mathbf{w}}(Z), \mathcal{D}_T(Z)) \right),$$

which completes the proof. ■

A.9 Proof of Lemma 3.2

Lemma 3.2. If *GLS* is verified, and if the confusion matrix \mathbf{C} is invertible, then $\mathbf{w} = \mathbf{C}^{-1}\boldsymbol{\mu}$.

Proof. Given (2), and with the joint hypothesis $\hat{Y} = h(Z)$ over both source and target domains, it is straightforward to see that the induced conditional distributions over predicted labels match between the source and target domains, i.e.:

$$\begin{aligned} \mathcal{D}_S(\hat{Y} = h(Z) \mid Y = y) &= \\ \mathcal{D}_T(\hat{Y} = h(Z) \mid Y = y), \forall y \in \mathcal{Y}. \end{aligned} \tag{17}$$

This allows us to compute $\boldsymbol{\mu}_{y'}$, $\forall y' \in \mathcal{Y}$ as

$$\begin{aligned} \mathcal{D}_T(\hat{Y} = y) &= \sum_{y' \in \mathcal{Y}} \mathcal{D}_T(\hat{Y} = y \mid Y = y') \cdot \mathcal{D}_T(Y = y') \\ &= \sum_{y' \in \mathcal{Y}} \mathcal{D}_S(\hat{Y} = y \mid Y = y') \cdot \mathcal{D}_T(Y = y') \\ &= \sum_{y' \in \mathcal{Y}} \mathcal{D}_S(\hat{Y} = y, Y = y') \cdot \frac{\mathcal{D}_T(Y = y')}{\mathcal{D}_S(Y = y')} \\ &= \sum_{y' \in \mathcal{Y}} \mathbf{C}_{y,y'} \cdot \mathbf{w}_{y'}. \end{aligned}$$

where we used (17) for the second line. We thus have $\boldsymbol{\mu} = \mathbf{C}\mathbf{w}$ which concludes the proof. ■

A.10 \mathcal{F} -IPM for Distributional Alignment

In Table 4, we list different instances of IPM with different choices of the function class \mathcal{F} in the above definition, including the total variation distance, Wasserstein-1 distance and the Maximum mean discrepancy (Gretton et al., 2012).

Table 4: List of IPMs with different \mathcal{F} . $\|\cdot\|_{\text{Lip}}$ denotes the Lipschitz seminorm and \mathcal{H} is a reproducing kernel Hilbert space (RKHS).

\mathcal{F}	$d_{\mathcal{F}}$
$\{f : \ f\ _{\infty} \leq 1\}$	Total Variation
$\{f : \ f\ _{\text{Lip}} \leq 1\}$	Wasserstein-1 distance
$\{f : \ f\ _{\mathcal{H}} \leq 1\}$	Maximum mean discrepancy

B Experimentation Details

B.1 Description of the domain adaptation tasks

Digits We follow a widely used evaluation protocol (Hoffman et al., 2017; Long et al., 2018). For the digits datasets MNIST (M, LeCun & Cortes (2010)) and USPS (U, Dheeru & Karra (2017)), we consider the DA tasks: $M \rightarrow U$ and $U \rightarrow M$. Performance is evaluated on the 10,000/2,007 examples of the MNIST/USPS test sets.

Visda (2017) is a sim-to-real domain adaptation task. The synthetic domain contains 2D rendering of 3D models captured at different angles and lighting conditions. The real domain is made of natural images. Overall, the training, validation and test domains contain 152,397, 55,388 and 5,534 images, from 12 different classes.

Office-31 (Saenko et al., 2010) is one of the most popular dataset for domain adaptation. It contains 4,652 images from 31 classes. The samples come from three domains: Amazon (A), DSLR (D) and Webcam (W), which generate six possible transfer tasks, $A \rightarrow D$, $A \rightarrow W$, $D \rightarrow A$, $D \rightarrow W$, $W \rightarrow A$ and $W \rightarrow D$, which we all evaluate.

Office-Home (Venkateswara et al., 2017) is a more complex dataset than Office-31. It consists of 15,500 images from 65 classes depicting objects in office and home environments. The images form four different domains: Artistic (A), Clipart (C), Product (P), and Real-World images (R). We evaluate the 12 possible domain adaptation tasks.

B.2 Full results on the domain adaptation tasks

Tables 5, 6, 7, 8, 9 and 10 show the detailed results of all the algorithms on each task of the domains described above. The subscript denotes the fraction of seeds for which our variant outperforms the base algorithm. More precisely, by outperform, we mean that for a given seed (which fixes the network initialization as well as the data being fed to the model) the variant has a larger accuracy on the test set than its base version. Doing so allows to assess specifically the effect of the algorithm, all else kept constant.

B.3 Jensen-Shannon divergence of the original and subsampled domain adaptation datasets

Tables 11, 12 and 13 show $D_{\text{JS}}(\mathcal{D}_S(Z) || \mathcal{D}_T(Z))$ for our four datasets and their subsampled versions, rows correspond to the source domain, and columns to the target one. We recall that subsampling simply consists in taking 30% of the first half of the classes in the source domain (which explains why $D_{\text{JS}}(\mathcal{D}_S(Z) || \mathcal{D}_T(Z))$ is not symmetric for the subsampled datasets).

Table 5: Results on the Digits tasks. M and U stand for MNIST and USPS, the prefix s denotes the experiment where the source domain is subsampled to increase $D_{JS}(\mathcal{D}_S^Y, \mathcal{D}_T^Y)$.

METHOD	M \rightarrow U	U \rightarrow M	AVG.		sM \rightarrow U	sU \rightarrow M	AVG.
NO AD.	79.04	75.30	77.17		76.02	75.32	75.67
DANN	90.65	95.66	93.15		79.03	87.46	83.24
IWDAN	93.28 _{100%}	96.52 _{100%}	94.90 _{100%}		91.77 _{100%}	93.32 _{100%}	92.54 _{100%}
IWDAN-O	93.73 _{100%}	96.81 _{100%}	95.27 _{100%}		92.50 _{100%}	96.42 _{100%}	94.46 _{100%}
CDAN	94.16	97.29	95.72		84.91	91.55	88.23
IWCDAN	94.36 _{60%}	97.45 _{100%}	95.90 _{80%}		93.42 _{100%}	93.03 _{100%}	93.22 _{100%}
IWCDAN-O	94.34 _{80%}	97.35 _{100%}	95.85 _{90%}		93.37 _{100%}	96.26 _{100%}	94.81 _{100%}

Table 6: Results on the Visda domain. The prefix s denotes the experiment where the source domain is subsampled to increase $D_{JS}(\mathcal{D}_S^Y, \mathcal{D}_T^Y)$.

METHOD	VISDA		sVISDA
NO AD.	48.39		49.02
DANN	61.88		52.85
IWDAN	63.52 _{100%}		60.18 _{100%}
IWDAN-O	64.19 _{100%}		62.10 _{100%}
CDAN	65.60		60.19
IWCDAN	66.49 _{60%}		65.83 _{100%}
IWCDAN-O	68.15 _{100%}		66.85 _{100%}
JAN	56.98 _{100%}		50.64 _{100%}
IWJAN	57.56 _{100%}		57.12 _{100%}
IWJAN-O	61.48 _{100%}		61.30 _{100%}

B.4 Losses

For batches of data (x_S^i, y_S^i) and (x_T^i) of size s , the DANN losses are:

$$\mathcal{L}_{DA}(x_S^i, y_S^i, x_T^i; \theta, \psi) = -\frac{1}{s} \sum_{i=1}^s \log(d_\psi(g_\theta(x_S^i))) + \log(1 - d_\psi(g_\theta(x_T^i))), \quad (18)$$

$$\mathcal{L}_C(x_S^i, y_S^i; \theta, \phi) = -\frac{1}{s} \sum_{i=1}^s \log(h_\phi(g_\theta(x_S^i)_{y_S^i})). \quad (19)$$

Similarly, the CDAN losses are:

$$\mathcal{L}_{DA}(x_S^i, y_S^i, x_T^i; \theta, \psi) = -\frac{1}{s} \sum_{i=1}^s \log(d_\psi(h_\phi(g_\theta(x_S^i)) \otimes g_\theta(x_S^i))) + \log(1 - d_\psi(h_\phi(g_\theta(x_T^i)) \otimes g_\theta(x_T^i))), \quad (20)$$

$$\mathcal{L}_C(x_S^i, y_S^i; \theta, \phi) = -\frac{1}{s} \sum_{i=1}^s \log(h_\phi(g_\theta(x_S^i)_{y_S^i})), \quad (21)$$

Table 7: Results on the Office dataset.

METHOD	A \rightarrow D	A \rightarrow W	D \rightarrow A	D \rightarrow W	W \rightarrow A	W \rightarrow D	AVG.
No DA	79.60	73.18	59.33	96.30	58.75	99.68	77.81
DANN	84.06	85.41	64.67	96.08	66.77	99.44	82.74
IWDAN	84.30 _{60%}	86.42 _{100%}	68.38 _{100%}	97.13 _{100%}	67.16 _{60%}	100.0 _{100%}	83.90 _{87%}
IWDAN-O	87.23 _{100%}	88.88 _{100%}	69.92 _{100%}	98.09 _{100%}	67.96 _{80%}	99.92 _{100%}	85.33 _{97%}
CDAN	89.56	93.01	71.25	99.24	70.32	100.0	87.23
IWCDAN	88.91 _{60%}	93.23 _{60%}	71.90 _{80%}	99.30 _{80%}	70.43 _{60%}	100.0 _{100%}	87.30 _{73%}
IWCDAN-O	90.08 _{60%}	94.52 _{100%}	73.11 _{100%}	99.30 _{80%}	71.83 _{100%}	100.0 _{100%}	88.14 _{90%}
JAN	85.94	85.66	70.50	97.48	71.5	99.72	85.13
IWJAN	87.68 _{100%}	84.86 _{60%}	70.36 _{60%}	98.98 _{100%}	70.06 _{60%}	100.0 _{100%}	85.32 _{60%}
IWJAN-O	89.68 _{100%}	89.18 _{100%}	71.96 _{100%}	99.02 _{100%}	73.0 _{100%}	100.0 _{100%}	87.14 _{100%}

Table 8: Results on the Subsampled Office dataset.

METHOD	sA \rightarrow D	sA \rightarrow W	sD \rightarrow A	sD \rightarrow W	sW \rightarrow A	sW \rightarrow D	AVG.
No DA	75.82	70.69	56.82	95.32	58.35	97.31	75.72
DANN	75.46	77.66	56.58	93.76	57.51	96.02	76.17
IWDAN	81.61 _{100%}	88.43 _{100%}	65.00 _{100%}	96.98 _{100%}	64.86 _{100%}	98.72 _{100%}	82.60 _{100%}
IWDAN-O	84.94 _{100%}	91.17 _{100%}	68.44 _{100%}	97.74 _{100%}	64.57 _{100%}	99.60 _{100%}	84.41 _{100%}
CDAN	82.45	84.60	62.54	96.83	65.01	98.31	81.62
IWCDAN	86.59 _{100%}	87.30 _{100%}	66.45 _{100%}	97.69 _{100%}	66.34 _{100%}	98.92 _{100%}	83.88 _{100%}
IWCDAN-O	87.39 _{100%}	91.47 _{100%}	69.69 _{100%}	97.91 _{100%}	67.50 _{100%}	98.88 _{100%}	85.47 _{100%}
JAN	77.74	77.64	64.48	91.68	92.60	65.10	78.21
IWJAN	84.62 _{100%}	83.28 _{100%}	65.30 _{80%}	96.30 _{100%}	98.80 _{100%}	67.38 _{100%}	82.61 _{97%}
IWJAN-O	88.42 _{100%}	89.44 _{100%}	72.06 _{100%}	97.26 _{100%}	98.96 _{100%}	71.30 _{100%}	86.24 _{100%}

where $h_\phi(g_\theta(x_S^i)) \otimes g_\theta(x_S^i) := (h_1(g(x_S^i))g(x_S^i), \dots, h_k(g(x_S^i))g(x_S^i))$ and $h_1(g(x_S^i))$ is the i -th element of vector $h(g(x_S^i))$.

The JAN losses (Long et al., 2017) are :

$$\mathcal{L}_{DA}(x_S^i, y_S^i, x_T^i; \theta, \psi) = -\frac{1}{s^2} \sum_{i,j=1}^s k(x_S^i, x_S^j) - \frac{1}{s^2} \sum_{i,j=1}^s k(x_T^i, x_T^j) + \frac{2}{s^2} \sum_{i,j=1}^s k(x_S^i, x_T^j) \quad (22)$$

$$\mathcal{L}_C(x_S^i, y_S^i; \theta, \phi) = -\frac{1}{s} \sum_{i=1}^s \log(h_\phi(g_\theta(x_S^i)_{y_S^i})), \quad (23)$$

where k corresponds to the kernel of the RKHS \mathcal{H} used to measure the discrepancy between distributions. Exactly as in Long et al. (2017), it is the product of kernels on various layers of the network $k(x_S^i, x_S^j) = \prod_{l \in \mathcal{L}} k^l(x_S^i, x_S^j)$. Each individual kernel k^l is computed as the dot-product between two transformations of the representation: $k^l(x_S^i, x_S^j) = \langle d_\psi^l(g_\theta^l(x_S^i)), d_\psi^l(g_\theta^l(x_S^j)) \rangle$ (in this case, d_ψ^l outputs vectors in a high-dimensional space). See Section B.6 for more details.

Table 9: Results on the Office-Home dataset.

METHOD	A \rightarrow C	A \rightarrow P	A \rightarrow R	C \rightarrow A	C \rightarrow P	C \rightarrow R	
No DA	41.02	62.97	71.26	48.66	58.86	60.91	
DANN	46.03	62.23	70.57	49.06	63.05	64.14	
IWDAN	48.65 _{100%}	69.19 _{100%}	73.60 _{100%}	53.59 _{100%}	66.25 _{100%}	66.09 _{100%}	
IWDAN-O	50.19 _{100%}	70.53 _{100%}	75.44 _{100%}	56.69 _{100%}	67.40 _{100%}	67.98 _{100%}	
CDAN	49.00	69.23	74.55	54.46	68.23	68.9	
IWCDAN	49.81 _{100%}	73.41 _{100%}	77.56 _{100%}	56.5 _{100%}	69.64 _{80%}	70.33 _{100%}	
IWCDAN-O	52.31 _{100%}	74.54 _{100%}	78.46 _{100%}	60.33 _{100%}	70.78 _{100%}	71.47 _{100%}	
JAN	41.64	67.20	73.12	51.02	62.52	64.46	
IWJAN	41.12 _{0%}	67.56 _{80%}	73.14 _{60%}	51.70 _{100%}	63.42 _{100%}	65.22 _{100%}	
IWJAN-O	41.88 _{80%}	68.72 _{100%}	73.62 _{100%}	53.04 _{100%}	63.88 _{100%}	66.48 _{100%}	
METHOD	P \rightarrow A	P \rightarrow C	P \rightarrow R	R \rightarrow A	R \rightarrow C	R \rightarrow P	AVG.
No DA	47.1	35.94	68.27	61.79	44.42	75.5	56.39
DANN	48.29	44.06	72.62	63.81	53.93	77.64	59.62
IWDAN	52.81 _{100%}	46.24 _{80%}	73.97 _{100%}	64.90 _{100%}	54.02 _{80%}	77.96 _{100%}	62.27 _{97%}
IWDAN-O	59.33 _{100%}	48.28 _{100%}	76.37 _{100%}	69.42 _{100%}	56.09 _{100%}	78.45 _{100%}	64.68 _{100%}
CDAN	56.77	48.8	76.83	71.27	55.72	81.27	64.59
IWCDAN	58.99 _{100%}	48.41 _{0%}	77.94 _{100%}	69.48 _{0%}	54.73 _{0%}	81.07 _{60%}	65.66 _{70%}
IWCDAN-O	62.60 _{100%}	50.73 _{100%}	78.88 _{100%}	72.44 _{100%}	57.79 _{100%}	81.31 _{80%}	67.64 _{98%}
JAN	54.5	40.36	73.10	64.54	45.98	76.58	59.59
IWJAN	55.26 _{80%}	40.38 _{60%}	73.08 _{80%}	64.40 _{60%}	45.68 _{0%}	76.36 _{40%}	59.78 _{63%}
IWJAN-O	57.78 _{100%}	41.32 _{100%}	73.66 _{100%}	65.40 _{100%}	46.68 _{100%}	76.36 _{20%}	60.73 _{92%}

The IWJAN losses are:

$$\mathcal{L}_{DA}^{\mathbf{w}}(x_S^i, y_S^i, x_T^i; \theta, \psi) = -\frac{1}{s^2} \sum_{i,j=1}^s \mathbf{w}_{y_S^i} \mathbf{w}_{y_S^j} k(x_S^i, x_S^j) - \frac{1}{s^2} \sum_{i,j=1}^s k(x_T^i, x_T^j) + \frac{2}{s^2} \sum_{i,j=1}^s \mathbf{w}_{y_S^i} k(x_S^i, x_T^j) \quad (24)$$

$$\mathcal{L}_C^{\mathbf{w}}(x_S^i, y_S^i; \theta, \phi) = -\frac{1}{s} \sum_{i=1}^s \frac{\mathbf{w}_{y_S^i}}{k\mathcal{D}_S(Y=y)} \log(h_\phi(g_\theta(x_S^i))_{y_S^i}). \quad (25)$$

B.5 Generation of domain adaptation tasks with varying $D_{JS}(\mathcal{D}_S(Z) \parallel \mathcal{D}_T(Z))$

We consider the MNIST \rightarrow USPS task and generate a set \mathcal{V} of 50 vectors in $[0.1, 1]^{10}$. Each vector corresponds to the fraction of each class to be trained on, either in the source or the target domain (to assess the impact of both). The left bound is chosen as 0.1 to ensure that classes all contain some samples.

This methodology creates 100 domain adaptation tasks, 50 for *subsampled*-MNIST \rightarrow USPS and 50 for MNIST \rightarrow *subsampled*-USPS, with Jensen-Shannon divergences varying from $6.1\text{e}-3$ to $9.53\text{e}-2^8$. They are then used to evaluate our algorithms, see Section 4 and Figures 1 and 2. Fig 2 shows the absolute performance of the 6 algorithms we consider here. We see the sharp decrease in performance of the base

⁸We manually rejected some samples to guarantee a rather uniform set of divergences.

Table 10: Results on the subsampled Office-Home dataset.

METHOD	$A \rightarrow C$	$A \rightarrow P$	$A \rightarrow R$	$C \rightarrow A$	$C \rightarrow P$	$C \rightarrow R$	
No DA	35.70	54.72	62.61	43.71	52.54	56.62	
DANN	36.14	54.16	61.72	44.33	52.56	56.37	
IWDAN	39.81 _{100%}	63.01 _{100%}	68.67 _{100%}	47.39 _{100%}	61.05 _{100%}	60.44 _{100%}	
IWDAN-O	42.79 _{100%}	66.22 _{100%}	71.40 _{100%}	53.39 _{100%}	61.47 _{100%}	64.97 _{100%}	
CDAN	38.90	56.80	64.77	48.02	60.07	61.17	
IWCDAN	42.96 _{100%}	65.01 _{100%}	71.34 _{100%}	52.89 _{100%}	64.65 _{100%}	66.48 _{100%}	
IWCDAN-O	45.76 _{100%}	68.61 _{100%}	73.18 _{100%}	56.88 _{100%}	66.61 _{100%}	68.48 _{100%}	
JAN	34.52	56.86	64.54	46.18	56.84	59.06	
IWJAN	36.24 _{100%}	61.00 _{100%}	66.34 _{100%}	48.66 _{100%}	59.92 _{100%}	61.88 _{100%}	
IWJAN-O	37.46 _{100%}	62.68 _{100%}	66.88 _{100%}	49.82 _{100%}	60.22 _{100%}	62.54 _{100%}	
METHOD	$P \rightarrow A$	$P \rightarrow C$	$P \rightarrow R$	$R \rightarrow A$	$R \rightarrow C$	$R \rightarrow P$	AVG.
No DA	44.29	33.05	65.20	57.12	40.46	70.0	
DANN	44.58	37.14	65.21	56.70	43.16	69.86	51.83
IWDAN	50.44 _{100%}	41.63 _{100%}	72.46 _{100%}	61.00 _{100%}	49.40 _{100%}	76.07 _{100%}	57.61 _{100%}
IWDAN-O	56.05 _{100%}	43.39 _{100%}	74.87 _{100%}	66.73 _{100%}	51.72 _{100%}	77.46 _{100%}	60.87 _{100%}
CDAN	49.65	41.36	70.24	62.35	46.98	74.69	56.25
IWCDAN	54.87 _{100%}	44.80 _{100%}	75.91 _{100%}	67.02 _{100%}	50.45 _{100%}	78.55 _{100%}	61.24 _{100%}
IWCDAN-O	59.63 _{100%}	46.98 _{100%}	77.54 _{100%}	69.24 _{100%}	53.77 _{100%}	78.11 _{100%}	63.73 _{100%}
JAN	50.64	37.24	69.98	58.72	40.64	72.00	53.94
IWJAN	52.92 _{100%}	37.68 _{100%}	70.88 _{100%}	60.32 _{100%}	41.54 _{100%}	73.26 _{100%}	55.89 _{100%}
IWJAN-O	56.54 _{100%}	39.66 _{100%}	71.78 _{100%}	62.36 _{100%}	44.56 _{100%}	73.76 _{100%}	57.36 _{100%}

versions DANN and CDAN. Comparatively, our importance-weighted algorithms maintain good performance even for large divergences between the marginal label distributions.

B.6 Implementation details

For MNIST and USPS, the architecture is akin to LeNet (LeCun et al., 1998), with two convolutional layers, ReLU and MaxPooling, followed by two fully connected layers. The representation is also taken as the last hidden layer, and has 500 neurons. The optimizer for those tasks is SGD with a learning rate of 0.02, annealed by 0.5 every five training epochs for $M \rightarrow U$ and 6 for $U \rightarrow M$. The weight decay is also $5e-4$ and the momentum 0.9.

For the Office and Visda experiments with IWDAN and IWCDAN, we train a ResNet-50, optimized using SGD with momentum. The weight decay is also $5e-4$ and the momentum 0.9. The learning rate is $3e-4$ for the Office-31 tasks $A \rightarrow D$ and $D \rightarrow W$, $1e-3$ otherwise (default learning rates from the CDAN implementation⁹).

For the IWJAN experiments, we use the default implementation of Xlearn codebase¹⁰ and simply add the weights estimation and reweighted objectives to it, as described in Section B.4. Parameters, configuration and

⁹<https://github.com/thuml/CDAN/tree/master/pytorch>

¹⁰<https://github.com/thuml/Xlearn/tree/master/pytorch>

Table 11: Jensen-Shannon divergence between the label distributions of the Digits and Visda tasks.

(A) FULL DATASET				(B) SUBSAMPLED			
	MNIST	USPS	REAL		MNIST	USPS	REAL
MNIST	0	6.64e−3	-	MNIST	0	6.52e−2	-
USPS	6.64e−3	0	-	USPS	2.75e−2	0	-
SYNTH.	-	-	2.61e−2	SYNTH.	-	-	6.81e−2

Table 12: Jensen-Shannon divergence between the label distributions of the Office-31 tasks.

(A) FULL DATASET			
	AMAZON	DSLR	WEBCAM
AMAZON	0	1.76e−2	9.52e−3
DSLR	1.76e−2	0	2.11e−2
WEBCAM	9.52e−3	2.11e−2	0

(B) SUBSAMPLED			
	AMAZON	DSLR	WEBCAM
AMAZON	0	6.25e−2	4.61e−2
DSLR	5.44e−2	0	5.67e−2
WEBCAM	5.15e−2	7.05e−2	0

networks remain the same.

Finally, for the Office experiments, we update the importance weights \mathbf{w} every 15 passes on the dataset (in order to improve their estimation on small datasets). On Digits and Visda, the importance weights are updated every pass on the source dataset. Here too, fine-tuning that value might lead to a better estimation of \mathbf{w} and help bridge the gap with the oracle versions of the algorithms.

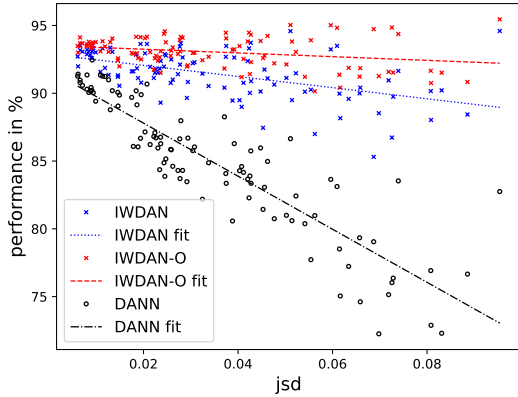
We use the `cvxopt` package¹¹ to solve the quadratic program 5.

¹¹<http://cvxopt.org/>

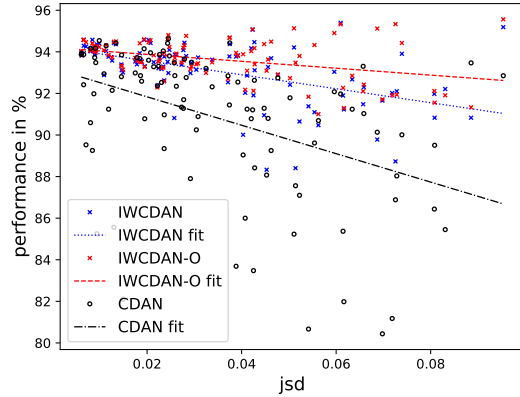
Table 13: Jensen-Shannon divergence between the label distributions of the Office-Home tasks.

(A) FULL DATASET				
	ART	CLIPART	PRODUCT	REAL WORLD
ART	0	3.85e−2	4.49e−2	2.40e−2
CLIPART	3.85e−2	0	2.33e−2	2.14e−2
PRODUCT	4.49e−2	2.33e−2	0	1.61e−2
REAL WORLD	2.40e−2	2.14e−2	1.61e−2	0

(B) SUBSAMPLED				
	ART	CLIPART	PRODUCT	REAL WORLD
ART	0	8.41e−2	8.86e−2	6.69e−2
CLIPART	7.07e−2	0	5.86e−2	5.68e−2
PRODUCT	7.85e−2	6.24e−2	0	5.33e−2
REAL WORLD	6.09e−2	6.52e−2	5.77e−2	0



(a) Performance of DANN, IWDAN and IWDAN-O.



(b) Performance of CDAN, CDAN and IWCDAN.

Figure 2: Performance in % of our algorithms and their base versions. The x -axis represents $D_{JS}(\mathcal{D}_S^Y, \mathcal{D}_T^Y)$, the Jensen-Shannon distance between label distributions. Lines represent linear fits to the data. For both sets of algorithms, the larger the jsd, the larger the improvement.